[35] McDermott MF. TNF and TNFR biology in health and disease. Cell Mol Biol 2001;47:619–35.
[36] Medeiros R, Prediger RD, Passos GF, Pandolfo P, Duarte FS, Franco JL, et al. Connecting TNF-alpha signaling pathways to iNOS expression in a mouse model of Alzheimer's disease: relevance for the behavioral and synaptic deficits induced by amyloid beta protein. J Neurosci 2007;27:5394–404.
[37] Moreira AL, Sampaio EP, Zmuidzinas A, Frindt P, Smith KA, Kaplan G. Thalidomide exerts its inhibitory action on tumor necrosis factor alpha by enhancing mRNA degradation. J Exp Med 1993;177:1675–80.
[38] Mouri A, Noda Y, Hara H, Mizoguchi H, Tabira T, Nabeshima T. Oral vaccination with a viral vector containing Abeta cDNA attenuates age-related Abeta accumulation and memory deficits without causing inflammation in a mouse Alzheimer model. FASEB J 2007;21:2135–48.
[39] Nabeshima T, Nitta A. Memory impairment and neuronal dysfunction induced by β-amyloid protein in rats. Tohoku J Exp Med 1994;174:241–9.
[40] Nathan C, Calingasan N, Nezezon J, Ding A, Lucia MS, La Perle K, et al. Protection from Alzheimer's-like disease in the mouse by genetic ablation of inducible nitric oxide synthase. J Exp Med 2005;202:1163–9.
[41] Nitta A, Itoh A, Hasegawa T, Nabeshima T. β-Amyloid protein-induced Alzheimer's disease animal model. Neurosci Lett 1994;170:63–6.
[42] Olney JW, Wozniak DF, Farber NB. Excitotoxic neurodegeneration in Alzheimer disease. New hypothesis and new therapeutic strategies. Arch Neurol 1997;54:1234–40.
[43] Perry RT, Collins JS, Wiener H, Acton R, Go RC. The role of TNF and its receptors in Alzheimer's disease. Neurobiol Aging 2001;22:873–83.
[44] Pike CJ, Walencewicz-Wasserman AJ, Kosmoski J, Cribbs DH, Glabe CG, Cotman CW. Structure-activity analyses of Abeta peptides: contributions of the β25–35 region to aggregation and neurotoxicity. J Neurochem 1995;64:253–65.
[45] Praticò D, Clark CM, Liun F, Rokach J, Lee VY, Trojanowski JQ. Increase of brain oxidative stress in mild cognitive impairment: A possible predictor of Alzheimer's disease. Arch Neurol 2002;59:972–6.
[46] Reiter CD, Teng RJ, Beckman JS. Superoxide reacts with nitric oxide to nitrate tyrosine at physiological pH via peroxynitrite. J Biol Chem 2000;275:32460–6.
[47] Rodrigo J, Fernández-Vizarra P, Castro-Blanco S, Bentura ML, Nieto M, Gómez-Isla T, et al. Nitric oxide in the cerebral cortex of amyloid-precursor protein (SW) Tg2576 transgenic mice. Neuroscience 2004;128:73–89.
[48] Ryu JK, McLarnon JG. Thalidomide inhibition of perturbed vasculature and glial-derived tumor necrosis factor-alpha in an animal model of inflamed Alzheimer's disease brain. Neurobiol Dis 2007 [Epub ahead of print].
[49] Selkoe DJ. The molecular pathology of Alzheimer's disease. Neuron 1991;6:487–98.
[50] Selkoe DJ. Deciphering the genesis and fate of amyloid beta-protein yields novel therapies for Alzheimer disease. J Clin Invest 2002;110:1375–81.
[51] Shalit F, Sredni B, Rosenblatt-Bin H, Kazimirsky G, Brodie C, Huberman M. Beta-amyloid peptide induces tumor necrosis factor-alpha and nitric oxide production in murine macrophage cultures. Neuroreport 1997;8:3577–80.
[52] Shimazawa R, Sano H, Tanatani A, Miyachi H, Hashimoto Y. Thalidomide as a nitric oxide synthase inhibitor and its structural development. Chem Pharm Bull 2004;52:498–9.
[53] Smith MA, Perry G, Richey PL, Sayre LM, Anderson VE, Beal MF, et al. Oxidative damage in Alzheimer's. Nature 1996;382:120–1.
[54] Smith MA, Richey Harris PL, Sayre LM, Beckman JS, Perry G. Widespread peroxynitrite-mediated damage in Alzheimer's disease. J Neurosci 1997;17:2653–7.
[55] Taniguchi T, Tanaka M, Ikeda A, Momotani E, Sekikawa K. Failure of germinal center formation and impairment of response to endotoxin in tumor necrosis factor-alpha deficient mice. Lab Invest 1997;77:647–58.
[56] Tarkowski E, Andreasen N, Tarkowski A, Blennow K. Intrathecal inflammation precedes development of Alzheimer's disease. J Neurol Neurosurg Psychiat 2003;74:1200–5.
[57] Tohgi H, Abe T, Yamazaki K, Murata T, Ishizaki E, Isobe C. Alterations of 3 nitrotyrosine concentration in the cerebrospinal fluid during aging and in patients with Alzheimer's disease. Neurosci Lett 1999;269:52–4.
[58] Tran MH, Yamada K, Nakajima A, Mizuno M, He J, Kamei H, et al. Tyrosine nitration of a synaptic protein synaptophysin contributes to amyloid β-peptide-induced cholinergic dysfunction. Mol Psychiat 2003;8:407–12.
[59] Tran MH, Yamada K, Olariu A, Mizuno M, Ren XH, Nabeshima T. Amyloid beta-peptide induces nitric oxide production in rat hippocampus: association with cholinergic dysfunction and amelioration by inducible nitric oxide synthase inhibitors. FASEB J 2001;15:1407–9.
[60] Tweedie D, Sambamurti K, Greig NH. TNF-alpha inhibition as a treatment strategy for neurodegenerative disorders: new drug candidates and targets. Curr Alzheimer Res 2007;4:378–85.
[61] Vodovotz Y, Lucia MS, Flanders KC, Chesler L, Xie QW, Smith TW, et al. Inducible nitric oxide synthase in tangle-bearing neurons of patients with Alzheimer's disease. J Exp Med 1996;184:1425–33.
[62] Wada R, Tifft CJ, Proia RL. Microglial activation precedes acute neurodegeneration in Sandhoff disease and is suppressed by bone marrow transplantation. Proc Natl Acad Sci USA 2000;97:10954–9.
[63] Walsh DM, Selkoe DJ. Deciphering the molecular basis of memory failure in Alzheimer's disease. Neuron 2004;44:181–93.
[64] Wang Q, Rowan MJ, Anwyl R. β-Amyloid-mediated inhibition of NMDA receptor-dependent long-term potentiation induction involves activation of microglia and stimulation of inducible nitric oxide synthase and superoxide. J Neurosci 2004;24:6049–56.
[65] Wang Q, Wu J, Rowan MJ, Anwyl R. α-amyloid inhibition of long-term potentiation is mediated via tumor necrosis factor. Eur J Neurosci 2005;22:2827–32.
[66] Wyss-Coray T. Inflammation in Alzheimer disease: driving force, bystander or beneficial response? Nat Med 2006;12:1005–15.
[67] Xie Z, Wei M, Morgan TE, Fabrizio P, Han D, Finch CE, et al. Peroxynitrite mediates neurotoxicity of amyloid beta-peptide1-42 and lipopolysaccharide-activated microglia. J Neurosci 2002;22:3484–92.
[68] Zameer A, Schulz P, Wang MS, Sierks MR. Single chain Fv antibodies against the 25-35 Aβ fragments inhibit aggregation and toxicity of Aβ42. Biochemistry 2006;45:11532–9.
[69] Zeng C, Lee JT, Chen H, Chen S, Hsu CY, Xu J. Amyloid-β peptide enhances tumor necrosis factor-alpha-induced iNOS through neutral sphingomyelinase/ceramide pathway in oligodendrocytes. J Neurochem 2005;94:703–12.

Cell Transplantation, Vol. 17, pp. 223–229, 2008
Printed in the USA.

0963-6897/08 $90.00 + .00
E-ISSN 1555-3892
www.cognizantcommunication.com

Bcl-2 Protects Tubular Epithelial Cells From Ischemia Reperfusion Injury by Inhibiting Apoptosis

Chigure Suzuki,* Yoshitaka Isaka,*† Shigeomi Shimizu,‡ Yoshihide Tsujimoto,‡ Yoshitsugu Takabatake,* Takahito Ito,* Shiro Takahara,† and Enyu Imai*

*Department of Nephrology, Osaka University Graduate School of Medicine, Suita, Osaka, Japan
†Department of Advanced Technology for Transplantation, Osaka University Graduate School of Medicine, Suita, Osaka, Japan
‡Department of Post-Genomics & Diseases, Osaka University Graduate School of Medicine, Suita, Osaka, Japan

Ischemia followed by reperfusion leads to severe organ injury and dysfunction. Inflammation is considered to be the most important cause of graft dysfunction in kidney transplantation subjected to ischemia. The mechanism that triggers inflammation and renal injury after ischemia remains to be elucidated; however, cellular stress may induce apoptosis during the first hours and days after transplantation, which might play a crucial role in early graft dysfunction. Bcl-2 is known to inhibit apoptosis induced by the etiological factors promoting ischemia and reperfusion injury. Accordingly, we hypothesized that an augmentation of the anti-apoptotic factor Bcl-2 may thus protect tubular epithelial cells by inhibiting apoptosis, thereby ameliorating the subsequent tubulointerstitial injury. We examined the effects of Bcl-2 overexpression on ischemia-reperfusion (I/R) injury using Bcl-2 transgenic mice (Bcl-2 TG) and their wild-type littermates (WT). To investigate the effects of I/R injury, the left renal artery and vein were clamped for 45 min, followed by reperfusion for 0–96 h. Bcl-2 TG exhibited decreased active caspase protein in the tubular cells, which led to a reduction in TUNEL-positive apoptotic cells. Consequently, interstitial fibrosis and phenotypic changes were ameliorated in Bcl-2 TG. In conclusion, Bcl-2 augmentation protected renal tubular epithelial cells from I/R, and subsequent interstitial injury by inhibiting tubular apoptosis.

Key words: Bcl-2; Apoptosis; TGF-β; Ischemia-reperfusion injury

INTRODUCTION

Both clinical and experimental evidence suggests that ischemia-reperfusion (I/R) injury to kidney grafts may influence both early and late transplant function (23). Ischemia followed by reperfusion is closely related to the pathogenesis of early graft damage. Overall, ischemia in a kidney graft is the sum of possible transient warm ischemia during allograft removal from the donor and cold ischemia associated with preservation and storage (19). Reperfusion, which is critical to the viability of the organ, may also induce additional damage (15). Prolonged exposure of the donor kidney to warm and/or cold ischemia increases the incidence of delayed graft function upon transplantation and primes a programmed process within the kidney, which may lead to chronic and progressive lesions (18). Several studies have reported the initial I/R injury to possibly significantly affect the graft outcome, thus suggesting that the long-term graft function might improve by manipulating the early graft injury induced by I/R (8).

I/R injury at the renal level is characterized by apoptosis of tubular cells and interstitial inflammation. Renal ischemia induces tubular cell injury with decreasing levels of ATP, increasing levels of calcium, and an alteration in the membrane lipid and enzyme activity (7). Reperfusion of the ischemic organ exacerbates ischemic injury by producing cytotoxic oxygen species and free radicals (9). In addition, a deleterious role for the inflammatory response in I/R-induced organ damage has also been suggested by the enhanced expression of adhesion molecules and proinflammatory mediators (cytokines, chemokines), the activation of the complement system, the priming of the coagulation cascade, and the subsequent leukocyte infiltration (5,25).

Apoptosis is a precisely regulated process and the molecular regulation of cell death has recently been reported to originate with the *bcl-2* gene family. Bcl-2 is known to inhibit the apoptosis induced by etiological factors promoting ischemia and reperfusion injury (14). Bcl-2 allows clonal survival after cell stress is removed (14). More importantly, human *bcl-2*-gene transfection

Received February 5, 2007; accepted September 30, 2007.
Address correspondence to Yoshitaka Isaka, Department of Advanced Technology for Transplantation, Osaka University Graduate School of Medicine, Suita, Osaka 565-0871, Japan. Tel: +81-6-6879-3746; Fax: +81-6-6879-3749; E-mail: isaka@att.med.osaka-u.ac.jp

resulted in the prevention of hypoxic cell death in liver (24). Therefore, Bcl-2 is a good candidate to inhibit programmed cell death in the context of I/R injury. Organ treatment modalities, which may reduce the consequences of I/R injuries, are thus considered to play a critical role in increasing graft survival, particularly with the present shortage of donor organs.

Therefore, we investigated the effects of Bcl-2 overexpression on tubular apoptosis and subsequent tubulointerstitial damage after I/R injury, using *bcl-2* transgenic mice.

MATERIALS AND METHODS

Experimental Design

In order to confirm the protective effects of Bcl-2 on tubular epithelial cells, we employed Bcl-2 transgenic mice (Bcl-2 TG) harboring the human *bcl-2* gene (12). In this transgenic mouse, human *bcl-2* was driven by the regulatory sequences of the rat *L-type pyruvate kinase* gene, which encodes a glycolytic enzyme expressed mainly in hepatocytes, enterocytes, and proximal tubular cells. Three- to 4-month-old Bcl-2 TG or WT mice were maintained under standard conditions until the experiments were performed. All studies were performed in accordance with the principles of the Guidelines on Animal Experimentation of Osaka University. All mice were anesthetized with an IP injection of sodium pentobarbital (30 mg/kg). To investigate the effects of I/R injury, Bcl-2 TG or WT were allowed to stabilize for 30 min before being subjected to 45 min of bilateral renal occlusion using artery clips to clamp the renal pedicles. Occlusion was visually confirmed by a paling in the kidney color. Reperfusion was initiated by removing the artery clips and it was visually confirmed when blushing was noted. The mice were sacrificed at 3, 24, 48, and 96 h after reperfusion. The sham-operated mice were also sacrificed as normal controls. Left kidneys were harvested after perfusing with phosphate-buffered saline (PBS).

Antibodies

To identify myofibroblasts, we used anti-human α-smooth muscle actin (α-SMA) antibody (EPOS System: Dako, Hamburg, Germany). The localization of active caspase-3 protein expression was determined by immunohistochemistry using antiactive caspase antibody (1:250 dilution; Promega, Madison, WI). To evaluate the caspase activity by a Western blot analysis, we used caspase-3 antibody (1:1000 dilution; BD Biosciences San Jose, CA). To examine the mechanisms of interstitial fibrosis, a potent fibrogenic growth factor was examined using anti-TGF-β1 antibody (1:50 dilution; Santa Cruz Biotechnology, Santa Cruz, CA).

Morphology and Immunohistochemical Staining

Tissue samples were fixed in 4% (w/v) buffered paraformaldehyde (PFA) for 16 h and then were embedded in paraffin. Tissue sections (4 μm) were mounted on silane (2% 3-aminopropyltriethoxysilane)-coated slides (Muto Pure Chemicals, Tokyo, Japan), deparaffinized with xylene, and stained with periodic acid-Schiff (PAS) and Masson's Trichrome. Immunohistochemical staining was performed using the Envision system (Dako), according to the manufacturer's instructions. Endogenous peroxidase activity was blocked with 3% H_2O_2 for 5 min. The first antibodies were diluted in 1.5% goat serum albumin in PBS at specific concentrations as described above, and incubated for 24 h at 4°C. This was followed by incubation with suitable secondary antibodies. Antigen retrieval was performed for 2 min in preheated 10 mmol/L sodium citrate (pH 7) using a microwave oven.

Terminal Deoxynucleotidyltransferase-Mediated dUTP Nick End-Labeling (TUNEL) Staining

TUNEL staining was performed using the in situ Apoptosis Detection Kit (Takara Bio, Otsu, Japan), according to the manufacturer's instructions. Briefly, the sections were deparaffinized and subjected to antigen retrieval in preheated 10 mmol/L sodium citrate (pH 7) using a steamer for 40 min. They were then incubated with 3% H_2O_2 for 10 min, which was followed by incubation with TdT enzyme solution for 90 min at 37°C. The reaction was terminated by incubation in a stop/wash buffer for 30 min at 37°C.

Western Blot Analysis

The tissue specimen was homogenized in RIPA buffer (10 mM Tris, pH 7.4, 150 mM NaCl, 1% NP-40,1 mM EDTA) containing 1% SDS and sonicated. The lysate was centrifuged at 15,000 rpm for 10 min at 4°C and the supernatant was collected. The protein concentration in each renal tissue lysate was determined using a BCA protein assay kit (Pierce Biotechnology, Rockford, IL). The lysate was mixed with 0.5 volume of 5× SDS sample buffer and boiled for 15 min. Next, 20 μg of protein was loaded onto each lane and electrophoresed on a 15% SDS polyacrylamide gel, followed by blotting on a PVDF transfer membrane (Amersham Biosciences, UK). The filter was blocked with 5% (w/v) nonfat milk or 1% BSA in 10 mM Tris-buffered saline with 0.1% Tween-20 (TBS-T), followed by overnight incubation at 4°C with diluted primary antibodies in TBS-T or blocking buffer. After washing three times in TBS-T, the filter was incubated with secondary antibody (1:1000) (Cell Signaling) in TBS-T for 30 min at room temperature and developed to detect specific pro-

tein bands using ECL reagents (Amersham Bioscience Corp., Piscataway, NJ).

RESULTS

Effects on Histological Changes

To investigate the role of apoptosis on I/R-induced kidney injury, WT mice and Bcl-2 transgenic mice, in which human Bcl-2 is highly expressed in tubular epithelial cells (Fig. 1), were treated with I/R, and the morphological changes were assessed. PAS staining of the kidney sections obtained from WT at 48 h (Fig. 2a after I/R injury revealed marked disruption of normal tubular morphology, including the widespread degeneration of tubular architecture, tubular dilatation, swelling, and luminal congestion with loss of the brush border. Furthermore, interstitial fibrosis was observed at 96 h after I/R injury in WT (Fig. 2b). In contrast, Bcl-2 TG exhibited reduced severity with regard to the characteristic histological changes of I/R injury, including tubular atrophy (Fig. 2c). Importantly, Bcl-2 TG showed minimal interstitial fibrosis at 96 h after I/R injury (Fig. 2d), thus indicating that Bcl-2 dramatically inhibited I/R-induced kidney damage.

Effects on Interstitial Phenotypic Changes in Kidney After I/R Injury

In order to detect interstitial myofibroblasts, which are associated with interstitial damage and fibrosis, the expression of α-SMA was examined immunohistochemically. As shown in Figure 3, the interstitial expression of α-SMA increased at 96 h after I/R injury in WT, while it was significantly suppressed and limited to the blood vessels in Bcl-2 TG (Fig. 3b), which was consistent with the results obtained from PAS staining (Fig. 2).

Effects on Tubular Apoptosis in the I/R Injury Kidney

The inhibition of I/R-induced kidney injury by Bcl-2 overexpression proposed the possibility that apoptosis plays a crucial role in I/R injury. In fact, the number of TUNEL-positive, apoptotic cells increased among the tubular epithelial cells at 96 h after I/R injury in WT (Fig. 4a), and decreased in Bcl-2 TG (Fig. 4b). Consistently, the distribution of active caspase-3 was scattered in the tubular epithelial cells and in the interstitial area (Fig. 5a) in WT, and positively stained cells often showed the morphological changes of apoptosis (i.e., shrunken cells with condensed nuclei). In contrast, the active caspase-3-positive cells were little observed in Bcl-2 TG (Fig. 5b). Similar results were also observed when caspase-3 activation was assessed by a Western blot analysis (Fig. 5c). These data indicated that I/R of kidney induced apoptosis in tubular epithelial cells, which was markedly prevented by Bcl-2.

Effects on Interstitial Fibrosis in Kidney After I/R Injury

Finally, to evaluate the I/R-induced kidney injury, and to examine the correlation between apoptosis and kidney injury, the extent of interstitial fibrotic change in I/R kidneys was investigated by performing histological analysis using Masson's trichrome staining. The size of the fibrotic lesions in the interstitium was determined in stained sections. Kidney sections from WT at 96 h after I/R injury showed an expanded interstitium when compared with normal kidney (data not shown). In contrast, the interstitial fibrotic area was significantly suppressed in I/R kidneys from Bcl-2 TG.

As a smaller fibrotic area was observed in Bcl-2 TG, we examined the expression of TGF-β, a potent fibrotic growth factor, in I/R kidneys. Immunohistochemical

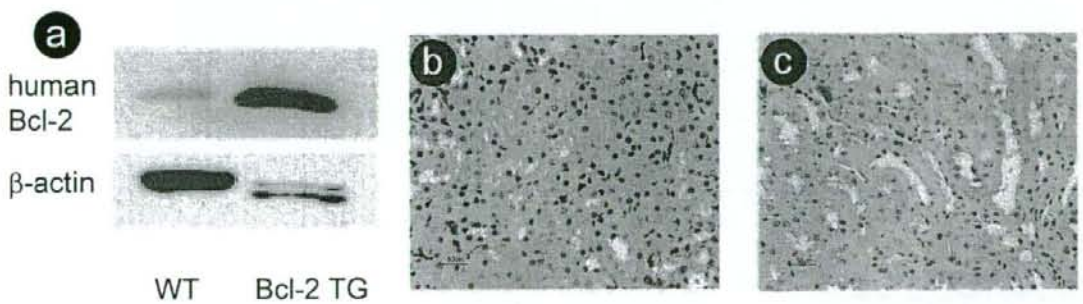

Figure 1. A Western blot analysis demonstrated that human Bcl-2 is highly expressed in Bcl-2 transgenic mice (a). Immunohistological staining showed that human Bcl-2 is not expressed in WT mice (b). Human Bcl-2 is expressed in tubular epithelial cells in Bcl-2 TG (c).

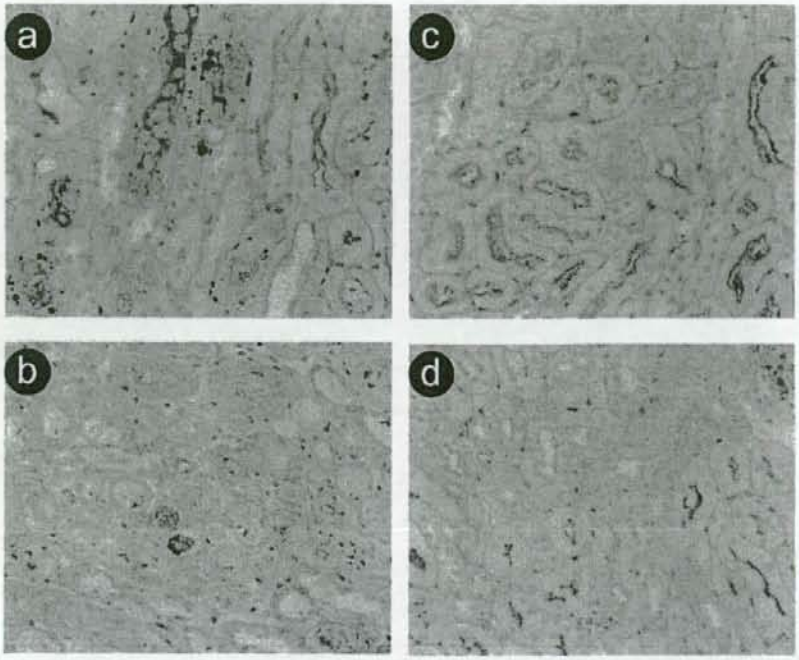

Figure 2. Representative morphological changes after PAS staining are shown in WT (a, b) and Bcl-2 TG (c, d) at 48 h (a, c) and 96 h (b, d) following I/R injury (original magnification 400×).

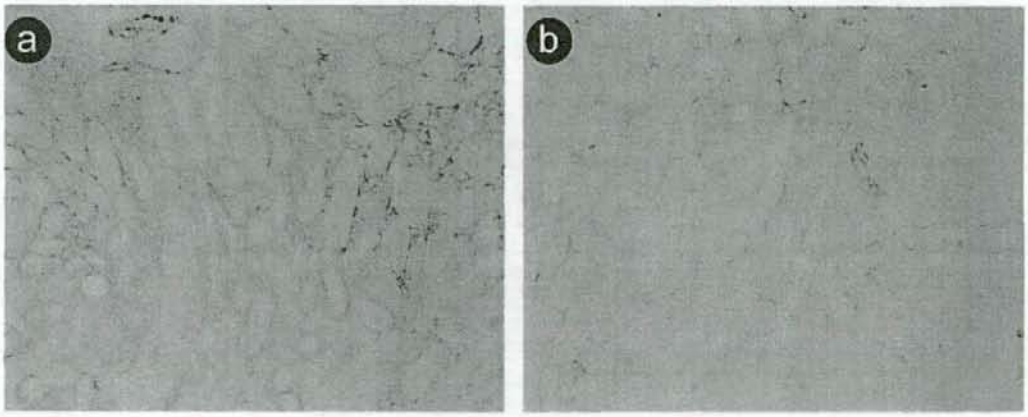

Figure 3. Effects of Bcl-2 on phenotypic alteration after I/R injury. α-SMA was strongly expressed in the interstitial area after I/R injury in WT (a), but was limited to blood vessels in Bcl-2 TG (b) (original magnification 400×).

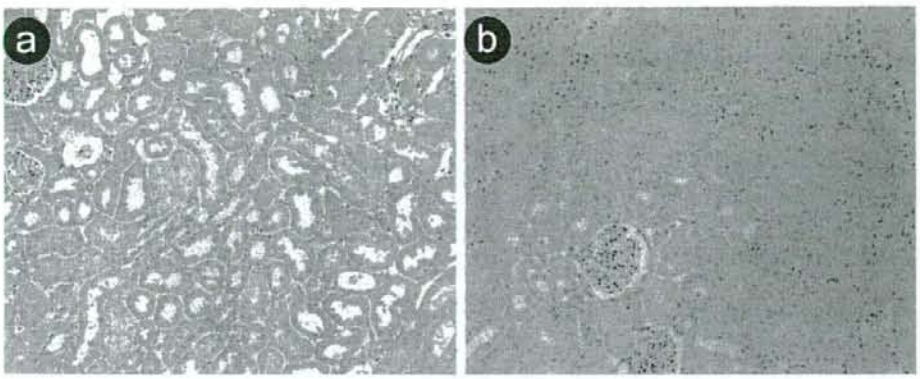

Figure 4. Effects of Bcl-2 on apoptosis at 96 h after I/R injury. Dark brown dots correspond to representative TUNEL-positive nuclei. (a) WT, (b) Bcl-2 TG (original magnification 400×).

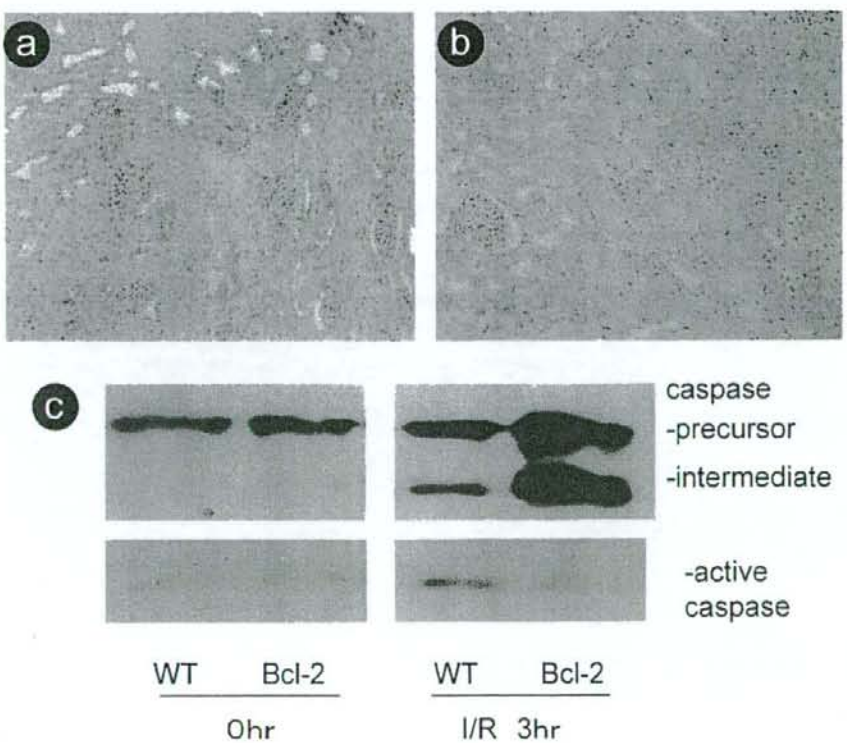

Figure 5. Effects of Bcl-2 on active caspase-3 expression at 3 h after I/R injury. Active caspase-3 was expressed in tubular epithelial cells at 3 h after I/R injury in WT (a), but not in Bcl-2 TG (b) (original magnification 400×). A Western blot analysis demonstrated that the active form of caspase-3 was diminished in Bcl-2 TG compared to WT.

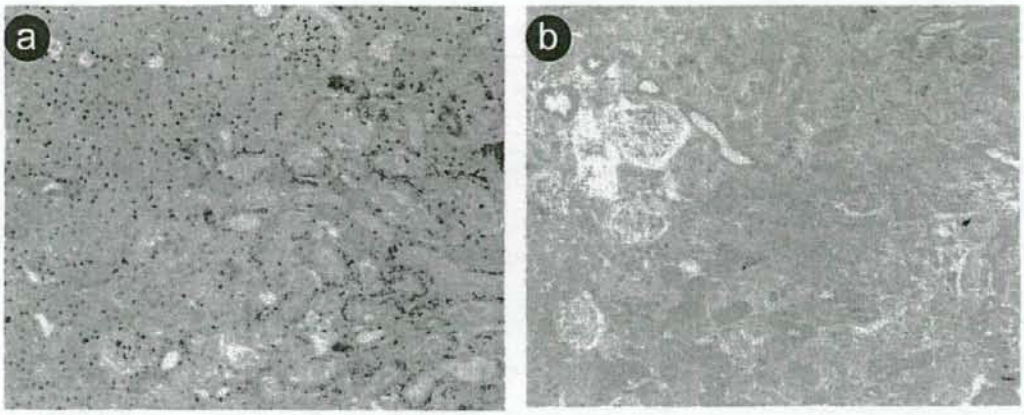

Figure 6. Effects of Bcl-2 on TGF-β expression. TGF-β was expressed in tubular epithelial cells after I/R injury in WT (a), but not in Bcl-2 TG (b) (original magnification 400×).

staining confirmed that the expression of TGF-β was upregulated in the tubular epithelial cells in I/R kidney from WT (Fig. 6a), and that this expression was weak in I/R kidney from Bcl-2 TG (Fig. 6b).

DISCUSSION

We examined whether Bcl-2 overexpression has a therapeutic effect on tubulointerstitial injury in a mouse model of I/R injury. We hypothesized that apoptosis following I/R constitutes a potential trigger of inflammation, and we studied this possibility by using Bcl-2 TG in a model of renal I/R. Evidence for the early involvement of apoptosis is provided by the characteristic morphological features in tubular epithelial cells, and the increase in TUNEL-positive cells, as well as increased active caspase-3 expression, in kidneys after I/R injury. These findings are in line with various in vivo and in vitro reports showing that renal apoptosis after ischemia is induced by hypoxia (1) and ATP depletion (13). Furthermore, during I/R-induced inflammation at day 1, upregulated Fas (16) and TNF-α (3) are associated with I/R-induced apoptosis. However, Bcl-2 TG exhibited decreased active caspase protein in tubular cells, and thus a reduction in the number of TUNEL-positive apoptotic cells. Consequently, both interstitial fibrosis and phenotypic changes were ameliorated in Bcl-2 TG.

Apoptosis represents a highly controlled process that is regulated by various factors (21). It is reported that Bcl-2 blocks cell death and modulates intracellular signaling events. In this regard, it has been shown that Bcl-2 inhibits depletion of Ca^{2+} from the endoplasmic reticulum (4) as well as the generation of reactive oxygen species and free radicals (10). Furthermore, it significantly impedes the downstream oxidative damage resulting from the radicals after they have been generated (11). An increase of mitochondrial membrane permeability is one of the key events in apoptotic death (20,22). The mitochondrial membrane permeability transition (MPT) is a Ca^{2+}-dependent increase of mitochondrial membrane permeability that leads to loss of $\Delta\psi$, mitochondrial swelling, and rupture of the outer mitochondrial membrane (26). The antiapoptotic Bcl-2 has the ability to block the MPT, and can therefore block MPT-dependent necrosis in addition to their well-established ability to inhibit apoptosis (20,22). As a result, the ability of Bcl-2 to protect against the damaging effects involved in ischemia and reperfusion injury makes Bcl-2 an appropriate candidate to inhibit apoptosis in renal transplantation.

We observed the upregulation of TGF-β in tubular epithelial cells in WT after I/R, as reported previously (6), while TGF-β expression was suppressed in Bcl-2 TG. Maintained upregulation of TGF-β expression is injurious, and is associated with the activation of fibroblasts and macrophages in the renal interstitium, and with the deposition of collagen and renal fibrosis (2). In addition, we observed α-SMA expression and fibrosis in the interstitium of WT after I/R injury, while α-SMA expression and fibrosis in the interstitium was suppressed in Bcl-2 TG. In our model, the precise relationship between Bcl-2 and tubulointerstitial injury remains unclear; however, one possible mechanism is that the Bcl-2-mediated protection from apoptosis results in the reduction of the TGF-β expression in tubular epithelial cells, which induces epithelial-mesenchymal transition (EMT) and subsequent α-SMA expression and interstitial fibrosis (17).

In line with previous findings, the results of this

study indicate that apoptosis occurs in kidneys after I/R, and this may therefore be an important phenomenon in clinical renal transplantation. Although the overexpression of Bcl-2 is not yet practicable in clinical settings, the augmentation of Bcl-2 in transplanted kidneys may be of therapeutic relevance for either minimizing or abolishing apoptotic cell death, thereby improving the outcome after kidney transplantation.

REFERENCES

1. Beeri, R.; Symon, Z.; Brezis, M.; Ben-Sasson, S. A.; Baehr, P. H.; Rosen, S.; Zager, R. A. Rapid DNA fragmentation from hypoxia along the thick ascending limb of rat kidneys. Kidney Int. 47(6):1806–1810; 1995.
2. Border, W. A.; Noble, N. A. TGF-beta in kidney fibrosis: A target for gene therapy. Kidney Int. 51(5):1388–1396; 1997.
3. Daemen, M. A.; van de Ven, M. W.; Heineman, E.; Buurman, W. A. Involvement of endogenous interleukin-10 and tumor necrosis factor-alpha in renal ischemia-reperfusion injury. Transplantation 67(6):792–800; 1999.
4. Foyouzi-Youssefi, R.; Arnaudeau, S.; Borner, C.; Kelley, W. L.; Tschopp, J.; Lew, D. P.; Demaurex, N.; Krause, K. H. Bcl-2 decreases the free Ca2+ concentration within the endoplasmic reticulum. Proc. Natl. Acad. Sci. USA 97(11):5723–5728; 2000.
5. Friedrichs, G. S.; Kilgore, K. S.; Manley, P. J.; Gralinski, M. R.; Lucchesi, B. R. Effects of heparin and N-acetyl heparin on ischemia/reperfusion-induced alterations in myocardial function in the rabbit isolated heart. Circ. Res. 75(4):701–710; 1994.
6. Gobe, G.; Zhang, X. J.; Willgoss, D. A.; Schoch, E.; Hogg, N. A.; Endre, Z. H. Relationship between expression of Bcl-2 genes and growth factors in ischemic acute renal failure in the rat. J. Am. Soc. Nephrol. 11(3):454–467; 2000.
7. Gulati, S.; Singh, A. K.; Irazu, C.; Orak, J.; Rajagopalan, P. R.; Fitts, C. T.; Singh, I. Ischemia-reperfusion injury: Biochemical alterations in peroxisomes of rat kidney. Arch. Biochem. Biophys. 295(1):90–100; 1992.
8. Hauet, T.; Goujon, J. M.; Vandewalle, A. To what extent can limiting cold ischaemia/reperfusion injury prevent delayed graft function? Nephrol. Dial. Transplant. 16(10): 1982–1985; 2001.
9. Kaminski, K. A.; Bonda, T. A.; Korecki, J.; Musial, W. J. Oxidative stress and neutrophil activation—the two keystones of ischemia/reperfusion injury. Int. J. Cardiol. 86(1):41–59; 2002.
10. Korsmeyer, S. J.; Shutter, J. R.; Veis, D. J.; Merry, D. E.; Oltvai, Z. N. Bcl-2/Bax: A rheostat that regulates an antioxidant pathway and cell death. Semin. Cancer Biol. 4(6): 327–332; 1993.
11. Kroemer, G. The proto-oncogene Bcl-2 and its role in regulating apoptosis. Nat. Med. 3(6):614–620; 1997.
12. Lacronique, V.; Mignon, A.; Fabre, M.; Viollet, B.; Rouquet, N.; Molina, T.; Porteu, A.; Henrion, A.; Bouscary, D.; Varlet, P.; Joulin, V.; Kahn, A. Bcl-2 protects from lethal hepatic apoptosis induced by an anti-Fas antibody in mice. Nat. Med. 2(1):80–86; 1996.
13. Lieberthal, W.; Menza, S. A.; Levine, J. S. Graded ATP depletion can cause necrosis or apoptosis of cultured mouse proximal tubular cells. Am. J. Physiol. 274(2 Pt. 2):F315–327; 1998.
14. Maulik, N.; Sasaki, H.; Galang, N. Differential regulation of apoptosis by ischemia-reperfusion and ischemic adaptation. Ann. NY Acad. Sci. 874:401–411; 1999.
15. Menger, M. D.; Pelikan, S.; Steiner, D.; Messmer, K. Microvascular ischemia-reperfusion injury in striated muscle: Significance of "reflow paradox". Am. J. Physiol. 263(6 Pt. 2):H1901–1906; 1992.
16. Nogae, S.; Miyazaki, M.; Kobayashi, N.; Saito, T.; Abe, K.; Saito, H.; Nakane, P. K.; Nakanishi, Y.; Koji, T. Induction of apoptosis in ischemia-reperfusion model of mouse kidney: Possible involvement of Fas. J. Am. Soc. Nephrol. 9(4):620–631; 1998.
17. Rhyu, D. Y.; Yang, Y.; Ha, H.; Lee, G. T.; Song, J. S.; Uh, S. T.; Lee, H. B. Role of reactive oxygen species in TGF-beta1-induced mitogen-activated protein kinase activation and epithelial-mesenchymal transition in renal tubular epithelial cells. J. Am. Soc. Nephrol. 16(3):667–675; 2005.
18. Terasaki, P. I.; Koyama, H.; Cecka, J. M.; Gjertson, D. W. The hyperfiltration hypothesis in human renal transplantation. Transplantation 57(10):1450–1454; 1994.
19. Tilney, N. L.; Guttmann, R. D. Effects of initial ischemia/reperfusion injury on the transplanted kidney. Transplantation 64(7):945–947; 1997.
20. Tsujimoto, Y.; Nakagawa, T.; Shimizu, S. Mitochondrial membrane permeability transition and cell death. Biochim. Biophys. Acta 1757(9–10):1297–1300; 2006.
21. Tsujimoto, Y.; Shimizu, S. Bcl-2 family: life-or-death switch. FEBS Lett. 466(1):6–10; 2000.
22. Tsujimoto, Y.; Shimizu, S. Role of the mitochondrial membrane permeability transition in cell death. Apoptosis 12(5):835–840; 2007.
23. Tullius, S. G.; Tilney, N. L. Both alloantigen-dependent and -independent factors influence chronic allograft rejection. Transplantation 59(3):313–318; 1995.
24. Yamabe, K.; Shimizu, S.; Kamiike, W.; Waguri, S.; Eguchi, Y.; Hasegawa, J.; Okuno, S.; Yoshioka, Y.; Ito, T.; Sawa, Y.; Uchiyama, Y.; Tsujimoto, Y.; Matsuda, H. Prevention of hypoxic liver cell necrosis by in vivo human bcl-2 gene transfection. Biochem. Biophys. Res. Commun. 243(1):217–223; 1998.
25. Zhou, W.; Farrar, C. A.; Abe, K.; Pratt, J. R.; Marsh, J. E.; Wang, Y.; Stahl, G. L.; Sacks, S. H. Predominant role for C5b-9 in renal ischemia/reperfusion injury. J. Clin. Invest. 105(10):1363–1371; 2000.
26. Zoratti, M.; Szabo, I. The mitochondrial permeability transition. Biochim. Biophys. Acta 1241(2):139–176; 1995.

Lysophosphatidylcholine as a death effector in the lipoapoptosis of hepatocytes[S]

Myoung Sook Han,[1,*] Sun Young Park,[1,*] Koei Shinzawa,[†] Sunshin Kim,[*] Kun Wook Chung,[*] Ji-Hyun Lee,[§] Choon Hyuck Kwon,[**] Kwang-Woong Lee,[**] Joon-Hyoek Lee,[*] Cheol Keun Park,[††] Woo Jin Chung,[§§] Jae Seok Hwang,[§§] Ji-Jing Yan,[***] Dong-Keun Song,[***] Yoshihide Tsujimoto,[†] and Myung-Shik Lee[2,*]

Departments of Medicine,[*] Surgery,[**] and Pathology,[††] Samsung Medical Center, Sungkyunkwan University School of Medicine, Seoul 135-710, Korea; Laboratory of Molecular Genetics,[†] Department of Medical Genetics, Osaka University Medical School and Solution Oriented Research for Science and Technology (SORST) of the Japan Science and Technology Corporation, Osaka 565-1871, Japan; Samsung Biomedical Research Institute,[§] Seoul 135-710, Korea; Department of Medicine,[§§] Keimyung University School of Medicine, Daegu 700-712, Korea; and Department of Pharmacology,[***] College of Medicine, Hallym University, Chunchon, Gangwon 200-702, Korea

Abstract **The pathogenesis of nonalcoholic steatohepatitis (NASH) is unclear, despite epidemiological data implicating FFAs. We studied the pathogenesis of NASH using lipoapoptosis models. Palmitic acid (PA) induced classical apoptosis of hepatocytes. PA-induced lipoapoptosis was inhibited by acyl-CoA synthetase inhibitor but not by ceramide synthesis inhibitors, suggesting that conversion products other than ceramide are involved. Phospholipase A_2 (PLA_2) inhibitors blocked PA-induced hepatocyte death, suggesting an important role for PLA_2 and its product lysophosphatidylcholine (LPC). Small interfering RNA for Ca^{2+}-independent phospholipase A_2 ($iPLA_2$) inhibited the lipoapoptosis of hepatocytes. PA increased LPC content, which was reversed by $iPLA_2$ inhibitors. Pertussis toxin or dominant-negative $G\alpha_i$ mutant inhibited hepatocyte death by PA or LPC acting through G-protein-coupled receptor (GPCR)/$G\alpha_i$. PA decreased cardiolipin content and induced mitochondrial potential loss and cytochrome *c* translocation. Oleic acid inhibited PA-induced hepatocyte death by diverting PA to triglyceride and decreasing LPC content, suggesting that FFAs lead to steatosis or lipoapoptosis according to the abundance of saturated/unsaturated FFAs. LPC administration induced hepatitis in vivo. LPC content was increased in the liver specimens from NASH patients. These results demonstrate that LPC is a death effector in the lipoapoptosis of hepatocytes and suggest potential therapeutic values of PLA_2 inhibitors or GPCR/$G\alpha_i$ inhibitors in NASH.**—Han, M. S., S. Y. Park, K. Shinzawa, S. Kim, K. W. Chung, J-H. Lee, C. H. Kwon, K-W. Lee, J-H. Lee, C. K. Park, W. J. Chung, J. S. Hwang, J-J. Yan, D-K. Song, Y. Tsujimoto, and M-S. Lee. **Lysophosphatidylcholine as a death effector in the lipoapoptosis of hepatocytes.** *J. Lipid Res.* **2008.** 49: **84–97.**

Supplementary key words fatty acids • phospholipase A_2 • steatohepatitis • triglyceride • ceramide

Nonalcoholic fatty liver disease (NAFLD) is characterized by lipid deposition in hepatocytes without alcohol abuse (1). Nonalcoholic steatohepatitis (NASH) is a severe form of NAFLD accompanied by necrosis, inflammation, and fibrosis (2). Although steatosis alone is nonprogressive, 20% of NASH progresses to cirrhosis (1). The pathogenesis of NAFLD is not clearly understood and may entail multiple injuries from increased FFAs, oxidative stress, lipid peroxidation, and tumor necrosis factor-α (1, 3).

NAFLD is frequently associated with type 2 diabetes, obesity, and insulin resistance, which constitute important components of the metabolic syndrome (2). FFAs released

Manuscript received 16 April 2007 and in revised form 14 September 2007 and in re-revised form 17 October 2007.

Published, JLR Papers in Press, October 18, 2007.
DOI 10.1194/jlr.M700184-JLR200

Abbreviations: A_{630}, absorption at 630 nm; ALT, alanine aminotransferase; AST, aspartate aminotransferase; BEL, bromoenol lactone; $cPLA_2$, cytoplasmic phospholipase A_2; DAG, diacylglycerol; GPCR, G-protein-coupled receptor; $iPLA_2$, Ca^{2+}-independent phospholipase A_2; JNK, c-Jun N-terminal kinase; LPA, lysophosphatidic acid; LPC, lysophosphatidylcholine; LPE, lysophosphatidylethanolamine; LPG, lysophosphatidylglycerol; LPI, lysophosphatidylinositol; LPS, lysophosphatidylserine; MAFP, methyl arachidonyl fluorophosphonate; MTT, 3-[4,5-dimethylthiazol-2-yl]-2,5-diphenyltetrazolium bromide; NAFLD, nonalcoholic fatty liver disease; NAO, 10-*N*-nonyl acridine orange; NASH, nonalcoholic steatohepatitis; OA, oleic acid; PA, palmitic acid; $PACOCF_3$, palmitoyl trifluoromethyl ketone; PC, phosphatidylcholine; PI, propidium iodide; PKC, protein kinase C; PLA_2, phospholipase A_2; PTX, pertussis toxin; siRNA, small interfering RNA; TG, triglyceride; TUNEL, terminal deoxynucleotidyl transferase mediated dUTP nick end labeling.

[1] M. S. Han and S. Y. Park contributed equally to this work.

[2] To whom correspondence should be addressed.
e-mail: mslee@smc.samsung.co.kr

[S] The online version of this article (available at http://www.jlr.org) contains supplementary data in the form of three figures.

from visceral fat of obese subjects are strong culprits in insulin resistance. Recent papers have suggested a potential role for FFAs in insulin deficiency as well as in insulin resistance, consistent with FFA-mediated injury of pancreatic β-cells and several other tissues (4).

FFAs may be related to NAFLD through their increased flux from visceral fat to the liver. Because of strong epidemiological and in vivo data suggesting the relationship between FFAs and NAFLD, several in vitro experiments studying hepatocyte injury by FFAs have been conducted, which suggested possible roles for the mitochondrial pathway, lysosomal pathway, endoplasmic reticulum stress, and c-Jun N-terminal kinase (JNK) activation in the lipoapoptosis of hepatocytes (5–9). However, the intracellular metabolites of FFAs that are directly responsible for such intracellular events are not clearly identified. We found evidence supporting the role of lysophosphatidylcholine (LPC) produced by phospholipase A_2 (PLA_2), which catalyzes the hydrolysis of the fatty acyl ester bond at the *sn*-2 position of glycerophospholipids and has been implicated in several types of cell death (10–13), as an effector in the lipoapoptosis of hepatocytes (**Fig. 1**).

MATERIALS AND METHODS

Reagents

Palmitoyl trifluoromethyl ketone ($PACOCF_3$) and methyl arachidonyl fluorophosphonate (MAFP) were from Calbiochem. zVAD-fmk was from Enzyme Systems (Livermore). All other chemicals were obtained from Sigma unless stated otherwise.

Cell death assay

Chang cells grown in DMEM-10% FBS were treated with FFAs or other reagents for 24 h unless stated otherwise. We chose a 24 h treatment protocol because our time course study revealed that cell death >50% with full-blown features of apoptosis, such as nuclear condensation/fragmentation and sub-G1 DNA peak, occurred at 24 h after treatment. Palmitic acid (PA) solution was made according to a previously published protocol with modifications (14). Briefly, PA stock solution (50 mM) was prepared by dissolving in 70% ethanol and heating at 50°C. Working PA solution was made by diluting stock solution in 2% fatty acid-free BSA-DMEM-10% FBS, because the concentration of FFAs, particularly that of PA, is quite low in 10% FBS, whereas cells were healthier with serum for prolonged experiments. 3-[4,5-Dimethylthiazol-2-yl]-2,5-diphenyltetrazolium bromide (MTT) assay, Hoechst 33258/propidium iodide (PI) staining, and DNA ploidy analysis were conducted as described (15). We used the MTT assay throughout the study because the results from the MTT assay were consistent with those of other cell death assays such as Hoechst/PI staining or DNA ploidy analysis in our pilot study. In some experiments, cells were pretreated with inhibitors for 1 h before PA treatment. To assess the death of primary murine hepatocytes, a lactate dehydrogenase release assay was used (12). Percentage cell death was calculated as (experimental release − spontaneous release)/(total release − spontaneous release) × 100.

Ammonia removal

Ammonia concentration in the culture supernatant was measured using a commercial kit (Asan Pharmaceuticals). Briefly, cells were incubated in a medium containing test reagents and 2 mM NH_4Cl for 48 h. The absorption at 630 nm (A_{630}) by indophenol generated from ammonia was measured. Percentage removal was calculated as [1 − (A_{630} with added ammonia to the

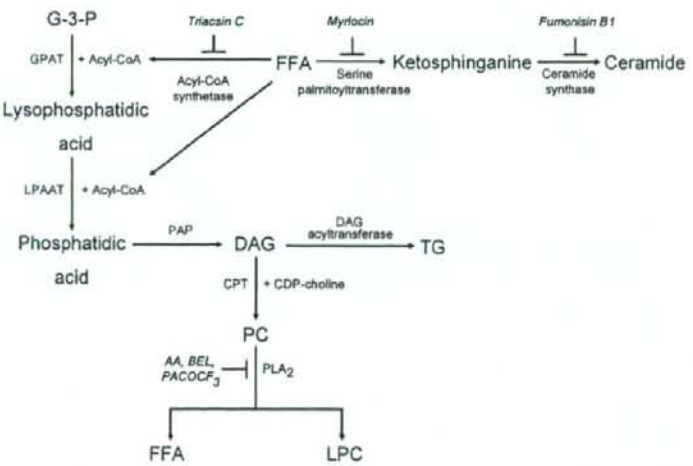

Fig. 1. Metabolism of FFAs. FFAs may be incorporated into ceramide, which could be an important death effector, or into diacylglycerol (DAG), which could be converted to lysophosphatidylcholine (LPC) or triglyceride (TG). AA, aristolochic acid; BEL, bromoenol lactone; CPT, CDP-choline:1,2-DAG phosphocholine transferase; G-3-P, glycerol-3-phosphate; GPAT, glycerophosphate acyltransferase; LPAAT, lysophosphatidic acid acyltransferase; PAP, phosphatidic acid phosphohydrolase; PC, phosphatidylcholine; $PACOCF_3$, palmitoyl trifluoromethyl ketone; PLA_2, phospholipase A_2.

cells − basal A_{630} of the cells)/(A_{630} with added ammonia to the blank − basal A_{630} of the blank)].

Small interfering RNA and RT-PCR

Small interfering RNAs (siRNAs) for human Ca^{2+}-independent phospholipase A_2 β (iPLA$_2$β) (AAT TGC GCG GAG AAC GAG GAG), iPLA$_2$γ (AAA ATG AAC ATT TCC GGG ACA), and an irrelevant siRNA purchased from Invitrogen were transfected using Oligofectamine (Invitrogen) according to the manufacturer's protocol. Expression of iPLA$_2$β and iPLA$_2$γ at the RNA level was determined by RT-PCR using specific primer sets. Expression of markers for hepatocytes was also tested by RT-PCR using specific primer sets (16).

Measurement of LPC

Intracellular LPC content was measured using an enzymatic assay reported previously (17). Briefly, sample was added to the mixture of 100 mM Tris-HCl, pH 8.0, 0.01% Triton X-100, 1 mM $CaCl_2$, 3 mM *N*-ethyl-*N*-[2-hydroxy-3-sulfopropyl]3-methylaniline, 10 U/ml peroxidase, 0.1 U/ml glycerophosphorylcholine phosphodiesterase, and 10 U/ml choline oxidase. After incubation at 37°C for 5 min, reagent mixture containing 100 mM Tris-HCl, pH 8.0, 5 mM 4-aminoantipyrine, 0.01% Triton X-100, and 20 U/ml lysophospholipase was added. After incubation for another 5 min, A_{570} was measured using LPC 16:0 as a standard.

Transfection

Chang cells stably expressing a dominant-negative $G\alpha_{i2}$ mutant (α_{i2}G203T) (18) or wild-type $G\alpha_{i2}$ (University of Missouri-Rolla cDNA Resource Center) were produced by transfection with FuGENE 6 (Roche) and selection with G418 for 3 weeks.

Mitochondrial events

After incubating cells with 0.4 μM 10-*N*-nonyl acridine orange (NAO; Molecular Probes) at 37°C, NAO fluorescence was measured by flow cytometry (19). Mitochondrial potential was measured by calculating A_{590}/A_{530} after incubating cells with 10 μg/ml JC-1 (Molecular Probes) for 10 min (20).

Cell fractionation

Cells lysed in an isotonic buffer were fractionated as described (20). The heavy membrane fraction and cytosolic fraction were subjected to Western blotting using specific antibodies against cytochrome *c* (PharMingen) or Bid (Santa Cruz) (15). The purity of the heavy membrane and cytosolic fractions was confirmed by Western blotting using anti-Cox4 and anti-IκB antibody, respectively. Expression of phosphorylated JNK and total JNK in the whole cell lysate was studied by Western blotting using specific antibodies (Cell Signaling).

Oil Red O staining

Cells were fixed with 10% formaldehyde for 1 h. After staining with 3 μg/ml Oil Red O solution for 15 min, dye was extracted by isopropanol and A_{540} was measured.

Human liver biopsy

Human liver tissue was obtained from the nontumor part of the livers from patients undergoing hepatic resection for metastatic colon cancer at Samsung Medical Center. The absence of cancer and cirrhosis was confirmed grossly and microscopically. The isolation of hepatocytes was performed using a two-step collagenase perfusion technique as described previously (21). After isolation, primary hepatocytes were cultured in a modified hormonally defined medium (William's E medium supplemented with 20 μg/l epidermal growth factor, 10 mg/l insulin, 1.7 mg/l hydrocortisone, 24.97 μg/l $CuSO_4 \cdot 5H_2O$, 14.38 pg/l $ZnSO_4 \cdot 7H_2O$, 3 μg/l H_2SeO_3, 50 mg/l linoleic acid, 1.05 g/l $NaHCO_3$, and 1.19 g/l HEPES) (22). Aspartate aminotransferase/alanine aminotransferase (AST/ALT) levels were measured using the FPC 3000 Blood Chemistry Analyzer (Fuji). Ultrasonography-guided liver biopsy was conducted in patients with clinical findings compatible with NAFLD without history of alcoholism (alcohol consumption < 140 g/week) using 18-gauge Solco needles inserted through the intercostal space. All patients had serum AST/ALT levels > 60 U/l and body mass index > 25 without recent history of diet control or parenteral nutrition. All were negative for viral markers, autoantibodies related to liver diseases, clinical evidence of cirrhosis, lipodystrophy, or Wilson's disease, and were not taking drugs related to lipid metabolism. Informed consent was obtained from all participants. All human studies were approved by the Institutional Review Board of Samsung Medical Center. An experienced hepatopathologist blinded to subject details scored the liver biopsy specimens according to a published classification (2).

Terminal deoxynucleotidyl transferase mediated dUTP nick end labeling staining

Terminal deoxynucleotidyl transferase mediated dUTP nick end labeling (TUNEL) staining of mouse liver tissues was conducted as described (15). Briefly, formalin-fixed sections were deparaffinized and microwaved in 0.01 M sodium citrate buffer (pH 6.0) and 0.1% Triton X-100. They were incubated with TUNEL reagents (Roche Molecular Biochemicals) at 37°C for 60 min. After washing, they were further incubated with Convert-POD for 30 min. Diaminobenzidine was used as a color substrate.

Mouse hepatocytes

Primary murine hepatocytes were isolated from C57BL/6 mice using the retrograde two-step collagenase perfusion technique (23). LPC (kindly provided by K-S. Song, Doosan Pharmaceutical; purity > 99%) dissolved in PBS-2% BSA by sonication was injected into the tail vein of ICR mice. All animal experiments were conducted in accordance with the institutional guidelines of the Osaka University Animal Facility and the Samsung Medical Center Animal Facility.

Measurement of iPLA$_2$ activity

Activity of iPLA$_2$ was measured using a commercial kit (Cayman) with modifications (24). Briefly, cells were collected with a cell scraper, sonicated, and centrifuged at 20,000 *g* at 4°C for 20 min. The supernatant was removed, and the concentration of proteins was determined. iPLA$_2$ activity was assayed by incubating the samples with arachidonoyl thio-PC for 1 h at 25°C in a Ca^{2+}-free buffer (300 mM NaCl, 0.5% Triton X-100, 60% glycerol, 4 mM EGTA, 10 mM HEPES, pH 7.4, and 2 mg/ml BSA). The reaction was terminated by adding 5,5′-dithio-bis-2-nitrobenzoic acid for 5 min, and A_{405} was measured. The specific activity of iPLA$_2$ was calculated and expressed as absorbance per milligram of protein. The background activity was subtracted from all readings.

Statistical analysis

All values are expressed as means ± SD from more than three independent experiments performed in triplicate. Two-tailed Student's *t*-test was used to compare values between two groups. ANOVA was used for multiple comparisons. The Scheffé test was used to compare two groups once ANOVA showed significant differences. $P < 0.05$ were considered to represent statistically significant differences.

RESULTS

Apoptosis of Chang liver cells by FFAs

We studied the effect of PA, the most abundant saturated fatty acid in vivo, on the Chang "normal" hepatocyte line. We chose Chang cells because they represent a more physiological system as nonmalignant human hepatocytes compared with hepatoma cells (25). RT-PCR analysis showed that Chang cells expressed markers for hepatocytes such as α-fetoprotein, ALT, phosphoenolpyruvate carboxykinase, albumin, tryptophan 2,3-dioxygenase, cytochrome enzymes (Cyp7A1, Cyp3A4), α-1-antitrypsin, and cytokeratin 8 (**Fig. 2A**) (16). Furthermore, Chang cells cleared 78.8% of added NH_4Cl, which was significantly higher than the clearance by control HeLa cells (8.0%) ($P < 0.05$) (Fig. 2A), suggesting that Chang cells represent authentic hepatocytes. PA induced Chang cell death, as assessed by MTT assay (Fig. 2B). Hoechst/PI staining demonstrated that Chang cell death by PA was a classical apoptosis characterized by nuclear condensation/fragmentation (Fig. 2C). Sub-G1 DNA peak was also observed by DNA ploidy analysis (Fig. 2D). A time course study showed that cell death >50% occurred at 24 h after treatment (Fig. 2E).

Because lipid intermediates produced from PA, such as ceramide, are well-known inducers of apoptosis (26), we investigated whether agents inhibiting the conversion of PA to lipid intermediates could affect Chang cell lipoapoptosis. Triacsin C, which inhibits acyl-CoA synthetase, the first enzyme in the conversion of PA to lipid intermediates through palmityol-CoA (27) (Fig. 1), effectively blocked Chang cell death by PA, suggesting that conversion products of PA but not PA itself induce lipoapoptosis ($P < 0.000005$) (Fig. 2F). We then studied the effect of fumonisin B1, which blocks ceramide synthesis by inhibiting sphingosine *N*-acyltransferase (Fig. 1) (28). Contrary to our expectation, fumonisin B1 did not affect Chang cell death by PA (Fig. 2G). Because this finding was inconsistent with previous reports by others using pancreatic islet cells (4), we next studied the effect of myriocin, which blocks the synthesis of ceramide/sphingosine by inhibiting serine palmitoyltransferase (29) (Fig. 1). Myriocin also did not inhibit Chang cell death by PA (Fig. 2H), suggesting that the conversion of FFAs to lipid intermediates in the sphingolipid-ceramide pathway and finally to ceramide is not involved in the lipoapoptosis of hepatocytes.

We next explored the possible involvement of protein kinase C (PKC) in Chang cell lipoapoptosis, because recent papers showed a role for PKC activation in apoptosis (30) and that PKC activators such as diacylglycerol (DAG) and LPC can be synthesized from palmitoyl-CoA (31) (Fig. 1). Both calphostin C and GF109203X, well-known PKC inhibitors, significantly attenuated Chang cell death by PA, supporting a role for PKC in Chang cell lipoapoptosis ($P < 0.000005$ for both) (see supplementary Fig. I).

Roles of PLA_2 and LPC in lipoapoptosis

We next studied the possible role of PLA_2 in Chang cell lipoapoptosis, because PLA_2 is involved in several cell death models (12, 13) and phosphatidylcholine (PC), a conversion product of DAG, can be a substrate for PLA_2, leading to the production of LPC, another PKC activator (Fig. 1). Intriguingly, aristolochic acid, a general inhibitor of PLA_2, and bromoenol lactone (BEL), a specific inhibitor of $iPLA_2$ (12, 13), markedly inhibited Chang cell death by PA, suggesting important roles for PLA_2 and the conversion products of PA downstream of PLA_2, rather than of DAG upstream of PLA_2, in lipoapoptosis and PKC activation ($P < 0.0001$ and 0.00005, respectively) (**Fig. 3A**). Because these results also suggested the possible involvement of $iPLA_2$ among diverse PLA_2 members, we used other PLA_2 inhibitors that are specific for each type of PLA_2. $PACOCF_3$, another $iPLA_2$-specific inhibitor of a different class (12, 32), dramatically blocked Chang cell death by PA ($P < 0.00005$). MAFP, an inhibitor of cytoplasmic phospholipase A_2 ($cPLA_2$) (12), also significantly blocked Chang cell death by PA ($P < 0.005$). However, the protection by the maximum tolerable MAFP level was less compared with that by $PACOCF_3$ ($P < 0.005$), suggesting that $iPLA_2$ rather than $cPLA_2$ is involved in the lipoapoptosis of hepatocytes (Fig. 3B). Consistent with these pharmacological data, $iPLA_2$ activity was increased significantly after treatment of Chang cells with PA ($P < 0.05$), which was inhibited by BEL ($P < 0.01$) (see supplementary Fig. II).

To confirm the role of $iPLA_2$, we conducted an RNA interference experiment. Transfection of siRNA for $iPLA_2\beta$ or $iPLA_2\gamma$, two major types of $iPLA_2$, significantly attenuated Chang cell death by PA, substantiating the roles of $iPLA_2$ in lipoapoptosis ($P < 0.00005$ for both comparisons) (Fig. 3C). Transfection of $iPLA_2\beta$ and $iPLA_2\gamma$ siRNA markedly decreased the expression of $iPLA_2\beta$ and $iPLA_2\gamma$, respectively, at the RNA level (Fig. 3D). However, the combination of both siRNAs did not induce a further decrease in lipoapoptosis (Fig. 3C).

Next, we studied whether LPC, which is liberated from PC by PLA_2 as the most abundant lysophospholipid in vivo, could indeed be produced from PA. Intracellular LPC content was increased significantly by PA ($P < 0.01$), and the LPC content after PA treatment was attenuated significantly by BEL ($P < 0.05$) (Fig. 3E). In contrast, LPC content in the culture supernatant was not increased after treatment of Chang cells with PA (see supplementary Fig. III). Treatment of Chang cells with exogenous palmitoyl-LPC (~10–50 μM) for 24 h also induced significant cell death in a dose-dependent manner ($P < 0.000001$) (Fig. 3F).

We next tested the effect of pertussis toxin (PTX) on Chang cell lipoapoptosis, because PTX inhibits LPC signaling through G-protein-coupled receptor (GPCR)/$G\alpha_i$ (33, 34). PTX (~100–400 ng/ml) remarkably inhibited Chang cell death by exogenous LPC or PA ($P < 0.00005$ and 0.000000005, respectively) (Fig. 3F). We further studied the role of GPCR/$G\alpha_i$ in lipoapoptosis by transfecting a dominant-negative mutant of $G\alpha_i$ ($\alpha_{i2}G203T$) (18). Stable Chang cell transfectants expressing $\alpha_{i2}G203T$ were resistant to death by PA or LPC, strongly supporting the role of LPC and GPCR/$G\alpha_i$ in lipoapoptosis of Chang cells (Fig. 3G). Transfection with a control wild-type $G\alpha_{i2}$ did

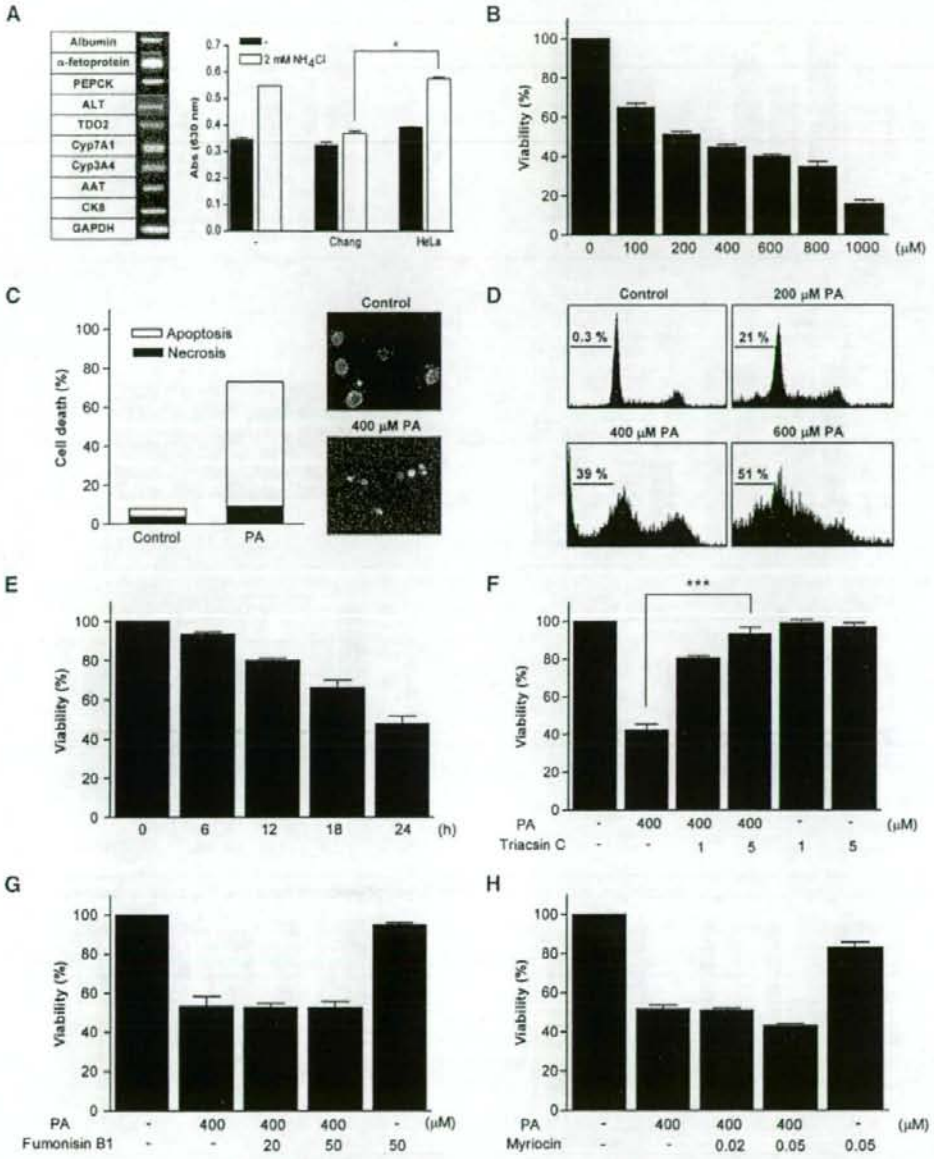

Fig. 2. Apoptosis of Chang liver cells by palmitic acid (PA). A: RT-PCR was conducted using RNA extracted from Chang "normal" liver cells and primers specific for various hepatocyte markers. Removal of exogenous ammonia by Chang cells or control HeLa cells was measured. AAT, α-1-antitrypsin; ALT, alanine aminotransferase; CK8, cytokeratin 8; PEPCK, phosphoenolpyruvate carboxykinase; TDO2, tryptophan 2,3-dioxygenase. B: Chang cells were treated with PA for 24 h, and 3-[4,5-dimethylthiazol-2-yl]-2,5-diphenyltetrazolium bromide (MTT) assay was conducted. C: After the same treatment as in B, Hoechst/propidium iodide (PI) double staining was performed, and the number of cells showing nuclear condensation/fragmentation was counted. D: After the same treatment as in B, DNA ploidy assay was conducted using PI staining followed by flow cytometric analysis. The percentage of cells showing sub-G1 peak was calculated as a measure of nuclear fragmentation. E: Chang cells were treated with PA for the indicated time periods, and MTT assay was performed. More than 50% of the cells died after treatment with 400 μM PA for 24 h. F: After pretreatment with triacsin C, an inhibitor of acyl-CoA synthetase, Chang cells were treated with PA for MTT assay. G, H: After pretreatment with fumonisin B1 or myriocin, inhibitors of ceramide synthesis, Chang cells were treated with PA. Values shown are means ± SD. * $P < 0.05$, *** $P < 0.001$.

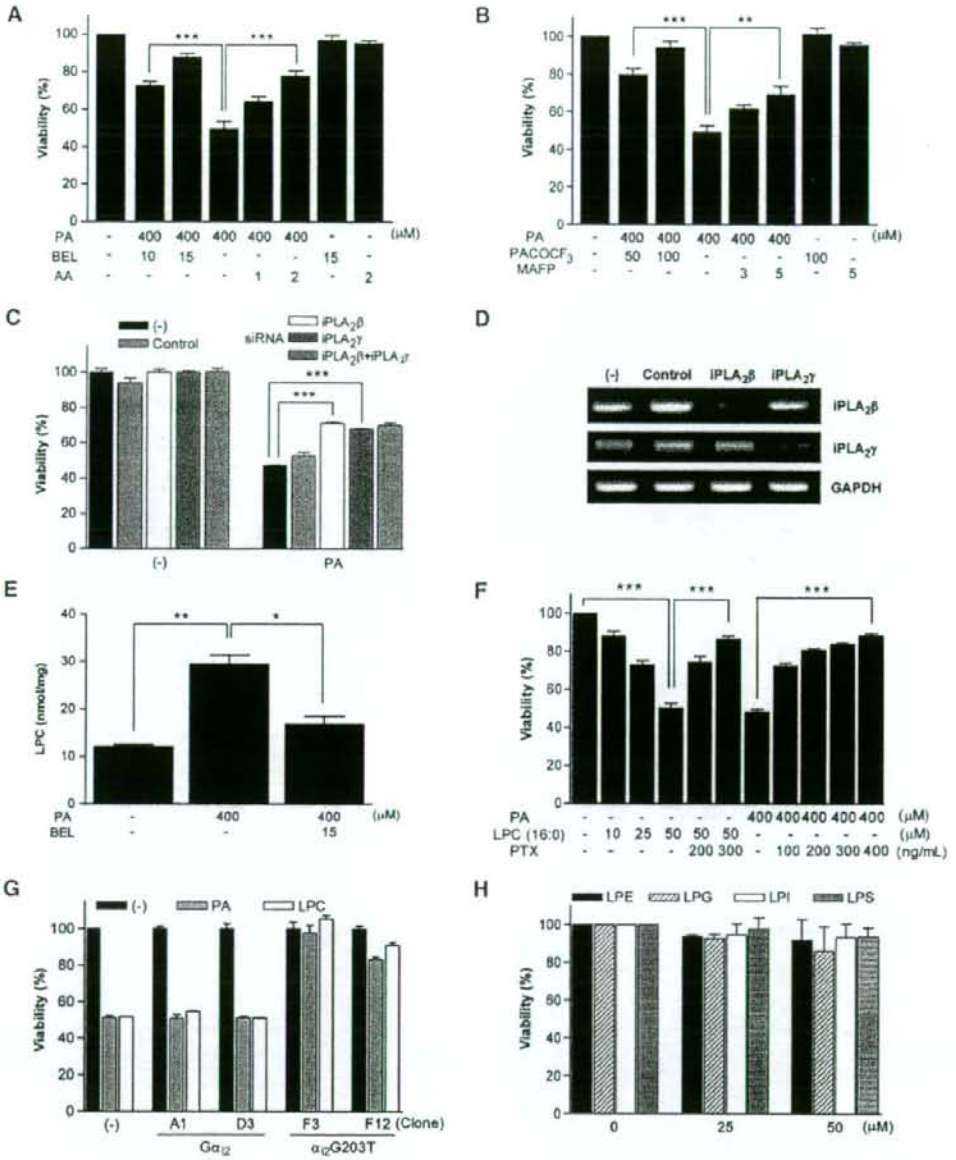

Fig. 3. Role of the PLA_2/LPC pathway in the lipoapoptosis of hepatocytes. A: After pretreatment with aristolochic acid (AA), a general inhibitor of PLA_2, or BEL, an inhibitor of Ca^{2+}-independent phospholipase A_2 (iPLA$_2$), Chang cells were treated with PA. After 24 h of incubation, MTT assay was done. B: Chang cells were pretreated with $PACOCF_3$, another iPLA$_2$-specific inhibitor, or methyl arachidonyl fluorophosphonate (MAFP), a cytoplasmic phospholipase A_2-specific inhibitor, before treatment with PA. The inhibition of lipoapoptosis by MAFP was less pronounced than that with $PACOCF_3$. C: Chang cells were transfected with iPLA$_2\beta$ and/or iPLA$_2\gamma$ small interfering RNA (siRNA) before treatment with PA. An irrelevant siRNA served as a control. D: Expression of iPLA$_2\beta$ and iPLA$_2\gamma$ in siRNA-transfected cells was examined by RT-PCR. E: After PA treatment with or without BEL pretreatment, intracellular LPC content in Chang cells was measured by an enzymatic assay. F: Chang cells were treated with exogenous LPC or PA with or without pertussis toxin (PTX) pretreatment, and cell viability was measured by MTT assay. G: Stable transfectants expressing wild-type $G\alpha_{i2}$ (A1, D3) or a dominant-negative $G\alpha_{i2}$ mutant (F3, F12) were produced by transfection with FuGENE 6 and G418 selection. They were treated with PA or LPC, and MTT assay was done. H: Chang cells were treated with minor products of iPLA$_2$ for 48 h. Values shown are means ± SD. * $P < 0.05$, ** $P < 0.01$, *** $P < 0.001$.

not significantly affect Chang cell death by PA or LPC, probably because of endogenous expression of $G\alpha_i$. We next examined the effect of other lysophospholipids that exist in vivo at much lower concentrations compared with LPC but that could be affected by PLA_2 inhibitors. Lysophosphatidylethanolamine (LPE), lysophosphatidylglycerol (LPG), lysophosphatidylinositol (LPI), or lysophosphatidylserine (LPS) up to 50 μM, which is much higher than their physiological concentrations, induced negligible cell death even at 48 h after treatment, suggesting that the effects of PLA_2 inhibitors are most likely through LPC (Fig. 3H).

We next studied intracellular events associated with lipoapoptosis. We measured the intracellular content of cardiolipin, which is crucial for cytochrome *c* binding to the mitochondrial inner membrane as a mitochondria-specific phospholipid and could be affected by FFA treatment. Cardiolipin content measured by NAO fluorescence began to decrease at ~3–6 h after PA treatment and decreased further at ~12–24 h after treatment (**Fig. 4A**). The PA-induced decrease in cardiolipin content was attenuated significantly by $iPLA_2$ inhibitors such as BEL and $PACOCF_3$, suggesting important roles for PLA_2 or LPC in the decrease of cardiolipin content and lipoapoptosis ($P < 0.0001$ and 0.0005, respectively) (Fig. 4B). We also studied whether LPC could directly induce changes in Bid apart from its receptor-mediated effect, because previous papers reported that Bid could perturb mitochondrial membrane in association with LPC (35). Bid in the mitochondrial fraction was increased by PA treatment, which was inhibited by BEL (Fig. 4C), suggesting a possible role for full-length Bid in cell death by LPC, as reported (35). Probably because of the decrease in cardiolipin content and the increase in Bid in the mitochondria, cytochrome *c* was translocated from mitochondria to cytoplasm and mitochondrial potential was decreased between 3 and 24 h after PA treatment (Fig. 4D). Chang cell death by PA was inhibited significantly by a pancaspase inhibitor, zVAD-fmk, suggesting that effector caspases were activated downstream of cytochrome *c* translocation ($P < 0.000005$) (Fig. 4E). We also studied whether PA activates JNK, because LPC is a well-known activator of JNK (36). Treatment of Chang cells with PA induced JNK activation, which was inhibited by $PACOCF_3$, suggesting that LPC produced from PA is involved in JNK activation (Fig. 4F). Exogenous LPC also induced JNK activation in Chang cells, as expected (Fig. 4F). Stable Chang cell transfectants expressing dominant-negative $\alpha_{i2}G203T$ mutant showed attenuated JNK activation after treatment with PA or LPC, suggesting that LPC produced from PA activates JNK through GPCR/$G\alpha_i$ (Fig. 4G). SP600125 (~10–20 μM), a JNK inhibitor, induced a small but significant decrease in PA-induced death (~25%) ($P < 0.005$), suggesting that JNK activation plays a certain role in the lipoapoptosis of Chang cells (Fig. 4H).

Inhibition of PA-induced lipoapoptosis by oleic acid

Because DAG can be converted to triglyceride (TG) (Fig. 1), we examined the role of TG in lipid injury. PA did not increase intracellular TG content, estimated by Oil Red O staining followed by spectrophotometry or microscopic examination. In contrast, oleic acid (OA), the most abundant unsaturated fatty acid in vivo, markedly increased TG content. Treatment with OA in combination with PA further increased TG content (**Fig. 5A, B**).

Regarding cell viability, OA did not induce Chang cell death. On the contrary, OA significantly blocked Chang cell death by PA ($P < 0.00005$), similar to previous reports (37) (Fig. 5C). OA also abolished the increase in LPC content by PA treatment ($P < 0.00005$) (Fig. 5D), suggesting that increased FFAs lead to either steatosis of hepatocytes attributable to increased TG content or death of hepatocytes attributable to increased LPC content, depending on the absolute/relative abundance of saturated/unsaturated fatty acids (Fig. 1).

Effect of PA on primary hepatocytes

We next used primary hepatocytes instead of cell lines. Hoechst/PI staining showed that PA induced the death of primary human hepatocytes as well, which was a classical apoptosis characterized by nuclear condensation/fragmentation (**Fig. 6A**). Lipoapoptosis of primary human hepatocytes by PA was inhibited by BEL ($P < 0.0005$) but not by fumonisin B1 or myriocin, suggesting that the $iPLA_2$/LPC pathway rather than the ceramide pathway is crucial, similar to Chang cells (Fig. 6B, C). Exogenous LPC also induced the death of primary human hepatocytes, which was inhibited by PTX ($P < 0.0005$) (Fig. 6D). PTX also significantly blocked the death of primary human hepatocytes by PA, suggesting that endogenous LPC induces the death of primary human hepatocytes through GPCR/$G\alpha_i$ ($P < 0.000001$) (Fig. 6D). OA attenuated the death of primary human hepatocytes by PA, supporting our hypothesis that unsaturated fatty acids divert saturated fatty acids into the TG pathway and attenuate primary human hepatocyte death by saturated fatty acids (Fig. 6E). Consistent with the death of primary human hepatocytes, PA induced the release of AST from cultured primary human hepatocytes, which was inhibited by BEL, PTX, or OA. LPC also induced AST release, which was blocked by PTX (Fig. 6F). PA induced the death of primary murine hepatocytes also, as assessed by lactate dehydrogenase release assay. Lipoapoptosis of primary murine hepatocytes by 750 μM PA (33.9 ± 3.8%) was significantly inhibited by 30 μM BEL (26.4 ± 3.6%), 100 μM $PACOCF_3$ (20.5 ± 3.1%), or 300 ng/ml PTX (26.9 ± 1.4%) ($P <$ 0.05, 0.01, and 0.05, respectively).

LPC content in NAFLD liver specimens

We next studied whether LPC is able to induce liver injury by directly injecting LPC in vivo. When 60 mg/kg LPC was administered to ICR mice through tail veins, AST/ALT levels were notably increased at 24 h after injection ($P < 0.005$ for both comparisons) (**Fig. 7A**). Hematoxylin and eosin and TUNEL staining of histological sections obtained at 3 days after LPC injection showed lobular hepatitis with a histological score of 1 (focal lytic necrosis, one focus or less per ×100 field) without evidence of steatosis (38) and $TUNEL^+$ apoptotic cells in the

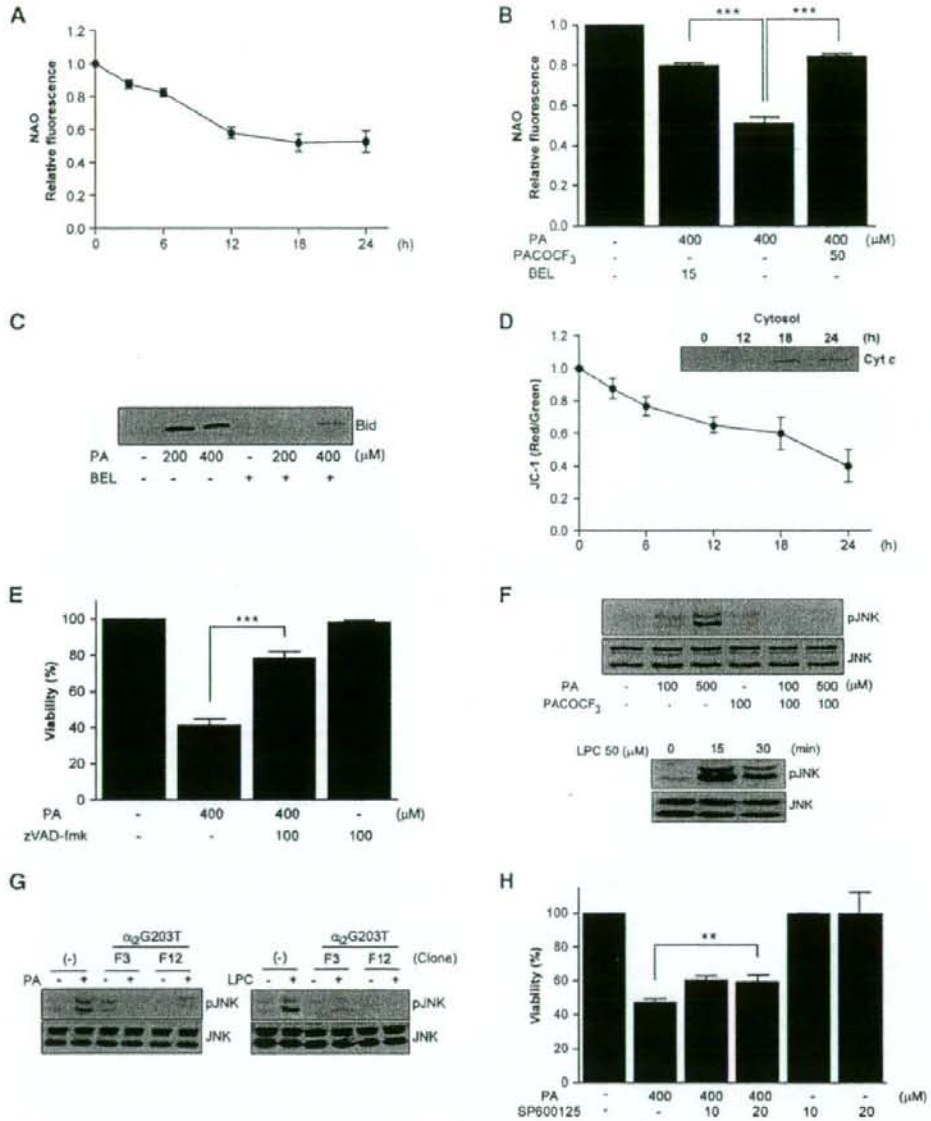

Fig. 4. Intracellular events associated with the lipoapoptosis of hepatocytes. A: Chang cells were treated with PA for the indicated time periods, and 10-*N*-nonyl acridine orange (NAO) fluorescence was determined by flow cytometry as a measure of mitochondrial cardiolipin content. B: Chang cells were treated with PA for 24 h after pretreatment with BEL or $PACOCF_3$, and NAO fluorescence was measured as in A. C: Chang cells were treated with PA with or without BEL pretreatment. After cell fractionation, the presence of Bid in the heavy membrane fraction was examined by Western blotting. D: Chang cells were treated with PA for the indicated time periods and then incubated with JC-1 for 10 min. Emission at 530 and 590 nm was measured, and absorption at 590 nm (A_{590})/A_{530} was calculated as an indicator of mitochondrial potential. Treated cells were fractionated, and the presence of cytochrome *c* in the cytosolic fraction was examined by Western blotting (inset). E: Chang cells were treated with PA after pretreatment with zVAD-fmk, and MTT assay was done. F: Chang cells were treated with PA for 24 h with or without $PACOCF_3$ pretreatment, and cell lysate was subjected to Western blotting using antibodies specific for phosphorylated c-Jun N-terminal kinase (JNK) or total JNK (upper panel). Chang cells were also treated with LPC for the indicated time, and cell lysate was subjected to Western blotting (lower panel). G: Stable transfectants expressing dominant-negative $G\alpha_{12}$ mutant were treated with PA or LPC, and cell lysate was subjected to Western blotting as in F. H: Chang cells were treated with PA after pretreatment with SP600125, a JNK inhibitor, and MTT assay was done. Values shown are means ± SD. ** $P < 0.01$, *** $P < 0.001$.

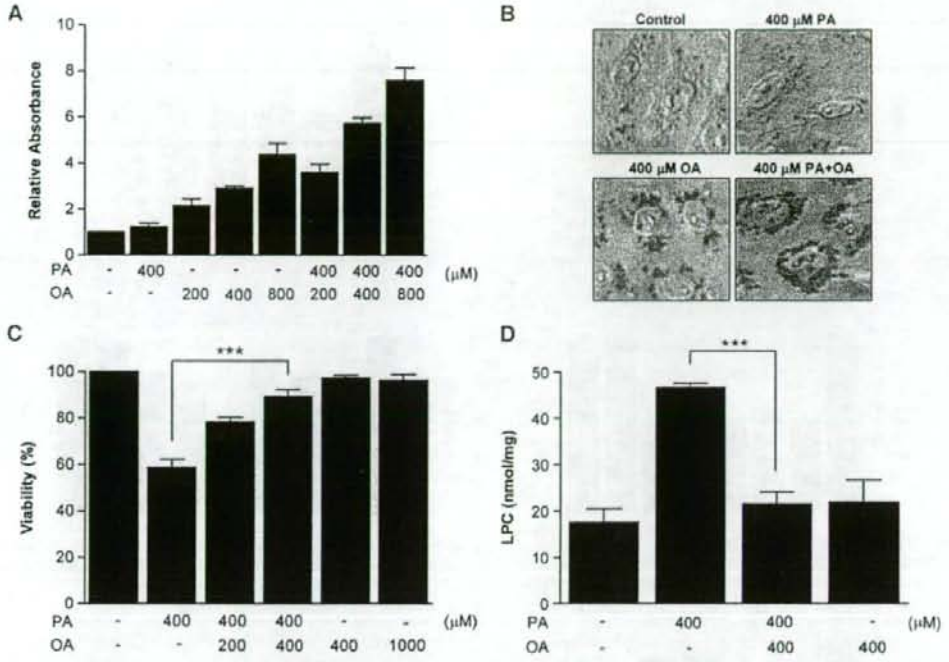

Fig. 5. Effect of unsaturated fatty acids on the lipoapoptosis of hepatocytes. A: Chang cells were treated with various combinations of saturated fatty acid (PA) and unsaturated fatty acid [oleic acid (OA)]. After Oil Red O staining and isopropanol extraction, A_{540} was measured to estimate intracellular TG content. B: After the same treatment and Oil Red O staining as in A, cells were observed with a light microscope. Treatment with OA but not with PA increased intracellular TG content. Combined OA/PA treatment further increased TG content. C: After treatment of Chang cells with various combinations of PA and OA, MTT assay was conducted. D: After the same treatment as in C, intracellular LPC content was measured by an enzymatic assay. Values shown are means ± SD. *** $P < 0.001$.

area of hepatitis, respectively, supporting our hypothesis that LPC plays a role as a mediator of hepatocyte injury in vivo (Fig. 7B).

We finally measured LPC content in liver biopsy specimens. ANOVA revealed that LPC content in the liver specimens from patients with NAFLD was significantly higher than that in the nontumor part of the liver from patients with metastatic colon cancer ($P < 0.005$). LPC content in the liver specimens from patients with NASH (NAFLD class 3–4) appears to be higher compared with that from patients with NAFLD class 2 (lobular hepatitis only); however, the difference was not statistically significant by the Scheffé test ($P > 0.1$) (Fig. 7C).

DISCUSSION

We observed that PA induces the apoptosis of hepatocytes through conversion to LPC, which led to the activation of GPCR, mitochondrial events, and JNK (**Fig. 8**). Although Chang cells and primary hepatocytes from mice or human all underwent apoptosis after treatment with PA, the susceptibility to lipoapoptosis was different, which could be attributable to differences in cell types, species, or the method of cell death assay. Although the identity of Chang cells has been questioned, recent papers have demonstrated the hepatocyte nature of Chang cells based on the expression of α-fetoprotein and albumin (39, 40), which was again supported by our results showing the expression of various markers for hepatocytes and the removal of ammonia by Chang cells. In contrast to our expectation, the conversion of PA to ceramide/sphingosine did not play a role in Chang cell lipoapoptosis, because both fumonisin B1 and myriocin inhibiting ceramide synthesis at two different steps did not block Chang cell lipoapoptosis. These results differ from previous findings suggesting essential roles for ceramide in the lipoapoptosis of pancreatic islet cells or hematopoietic cells (4, 41). However, papers reporting the ceramide-independent lipoapoptosis of various types of cells, including hepatocytes, have also been published (5, 7, 42, 43). These discrepancies might be attributable to differences in cell types or experimental conditions.

Instead of the ceramide pathway, conversion to DAG, PC, and then LPC appears to play an important role in Chang cell lipoapoptosis. Palmitoyl-CoA can be incorpo-

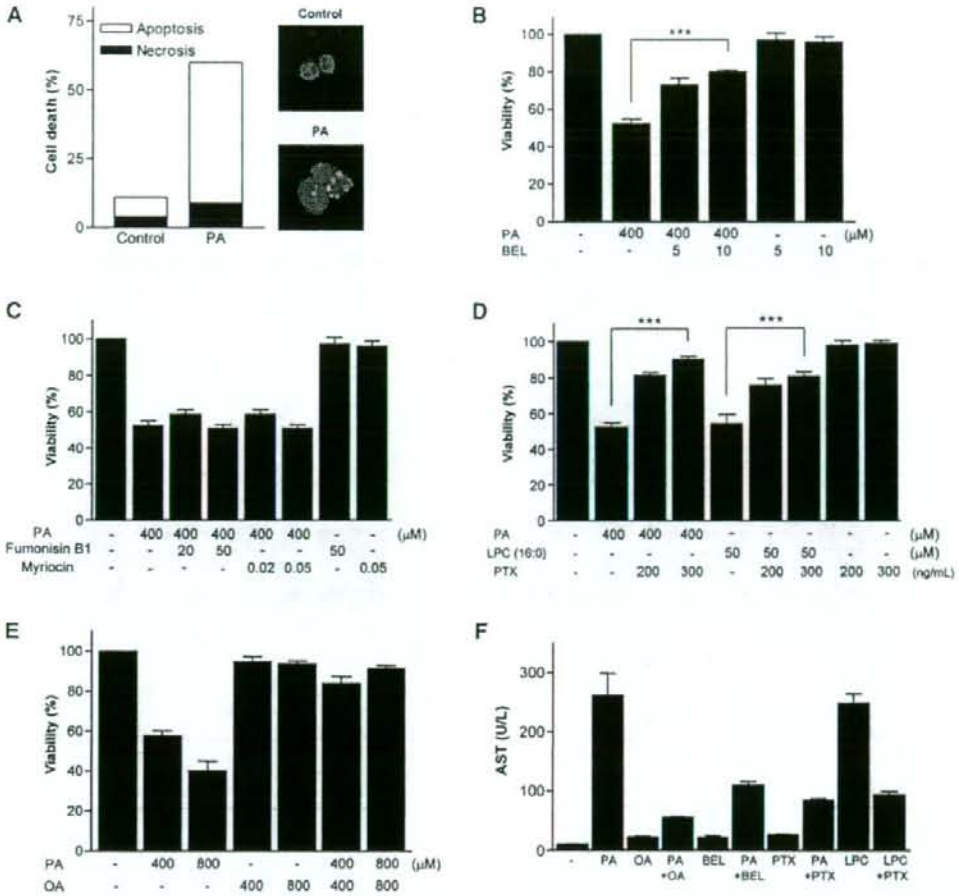

Fig. 6. Death of primary hepatocytes by PA. A: Primary human hepatocytes isolated by two-step collagenase perfusion were treated with PA for 24 h, and Hoechst/PI staining was conducted as in Fig. 2C. B: Primary human hepatocytes pretreated with BEL were incubated with PA as in Fig. 3A, and MTT assay was done. C: Primary human hepatocytes pretreated with fumonisin B1 or myriocin were incubated with PA as in Fig. 2G, H, and MTT assay was conducted. D: After pretreatment with PTX, primary human hepatocytes were treated with PA or exogenous LPC as in Fig. 3F. E: After treatment of primary human hepatocytes with various combinations of PA and OA, MTT assay was conducted as in Fig. 5C. F: After treatment of human primary hepatocytes with PA in the presence or absence of BEL, PTX, or OA, aspartate aminotransferase (AST) level in the supernatant was measured using a blood chemistry analyzer. Values shown are means ± SD. *** $P < 0.001$.

rated to phosphatidic acid, which can be converted to DAG, a well-known PKC activator (30) (Fig. 1). Downstream of DAG, we noticed that DAG could be converted to PC and then to LPC, another PKC activator, by PLA_2 (44). Because PLA_2 participates in several cell death models (12, 13), we investigated whether PLA_2 is involved in the lipoapoptosis of hepatocytes. Our results showing a remarkable inhibition of Chang cell lipoapoptosis by BEL or $PACOCF_3$ suggest the involvement of $iPLA_2$ and LPC rather than DAG upstream of PLA_2. Although BEL has been reported to inhibit phosphatidic acid phosphohydrolase in addition to $iPLA_2$ (24), our finding that another $iPLA_2$-specific inhibitor, $PACOCF_3$, which is structurally unrelated to BEL (24), dramatically inhibited Chang cell death by PA suggests that $iPLA_2$ plays a critical role in lipoapoptosis. Moreover, LPC content was increased significantly after PA treatment of Chang cells and reverted to a normal level with BEL, suggesting an important role of LPC as a death effector in PA-induced lipoapoptosis. However, it is not clear which among several types of $iPLA_2$ that could be inhibited by BEL (45, 46) is responsible for the lipoapoptosis of hepatocytes. Because we observed significant decreases in Chang cell lipoapoptosis with both $iPLA_2\beta$ and $iPLA_2\gamma$ siRNA, a single type of $iPLA_2$ may not

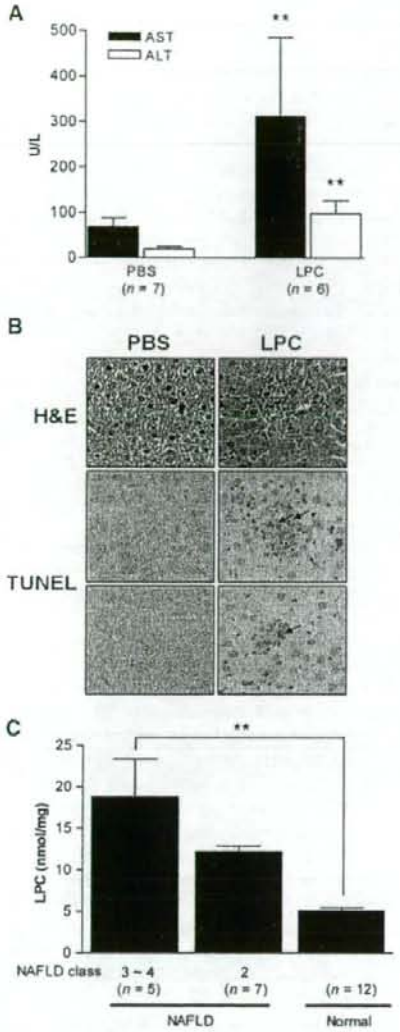

Fig. 7. LPC, liver injury in vivo, and nonalcoholic fatty liver disease (NAFLD). A: LPC was administered into the tail vein of ICR mice, and AST/ALT levels were measured. B: Histological grading of the liver injury was assessed according to a published criteria (38). TUNEL staining was done on the adjacent sections to identify apoptotic hepatocytes in the area of hepatitis. H&E, hematoxylin and eosin. Magnification ×100. C: LPC content was measured in liver biopsy specimens from patients with NAFLD and in the nontumoral part of the liver from patients undergoing hepatic resection for metastatic colon cancer (Normal). The severity of NAFLD was assessed according to a published classification (2). Values shown are means ± SD. ** $P < 0.01$.

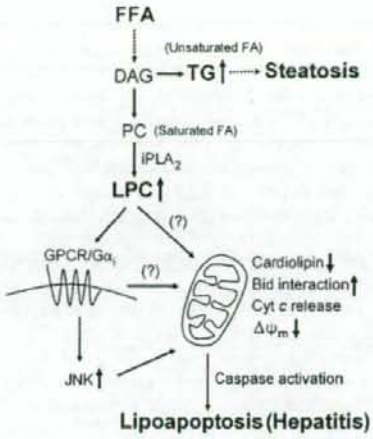

Fig. 8. Proposed model for NAFLD. DAG produced by the incorporation of FFA into the glycerol backbone may be converted to LPC or TG depending on the absolute/relative abundance of saturated/unsaturated fatty acids. Steatosis or hepatitis may occur when the TG pathway or the LPC pathway, respectively, prevails. LPC may induce apoptosis through the activation of G-protein-coupled receptor (GPCR/$G\alpha_i$), mitochondrial events, and JNK.

be fully responsible for the production of LPC from FFAs. Further work will be necessary to elucidate the roles of specific $iPLA_2$ types in lipoapoptosis.

The role of PLA_2 in cell death/survival has been reported in diverse models of hypoxia, reperfusion injury, and reactive oxygen species damage (12, 13, 47, 48). Our results are similar to previous findings showing a significant role of $iPLA_2$ in hypoxic cell injury (12, 47); however, our findings are different from those results in that LPC appears to be an effector downstream of $iPLA_2$ activation. Our data that $iPLA_2$ activity was significantly (nearly 2-fold) increased by PA and that the increased activity was completely reversed by BEL are also similar to previous data that $iPLA_2$ activity was increased in the course of hypoxic cell death (12). The mechanism of the activation of $iPLA_2$ activity by PA is not clearly understood and may involve translocation to target organelles, displacement of inhibitor molecules by FFA-induced endoplasmic reticulum stress, or reactive oxygen species (12, 24, 49). Incomplete protection of PA-induced hepatocyte death by a combination of $iPLA_2\beta$ and $iPLA_2\gamma$ siRNAs or $iPLA_2$ inhibitors such as BEL and $PACOCF_3$ suggests a potential role of $iPLA_2$-independent mechanisms in the lipoapoptosis of hepatocytes. For instance, the role of fatty acid metabolites other than LPC, such as DAG and ceramide, cannot be totally eliminated, because we used mostly pharmacological inhibitors that could have overlapping substrate specificities.

Exogenous LPC has been reported to induce apoptosis (44, 50) and stimulate inflammatory cells (17). However, the proapoptotic role of endogenous LPC has not been reported, to our knowledge. As $iPLA_2$ does not have a

specificity toward PC, the roles of other lysophospholipids cannot be completely eliminated. However, in vivo concentrations of other phospholipids, such as phosphatidylethanolamine, phosphatidylglycerol, phosphatidylinositol, and phosphatidylserine, are around or less than one-tenth of that of PC (51, 52). Much higher in vivo concentrations and much stronger apoptotic activity of LPC compared with LPE, LPG, LPI, or LPS essentially eliminates the possibility that other minor lysophospholipids play significant roles in lipoapoptosis. Previous papers also showed obvious apoptotic activity of LPC, whereas that of other lysophospholipids has not been clearly demonstrated (44, 50). Products of PLA_2 released from PC together with LPC, such as arachidonic acid or its derivatives (10, 11), have diverse effects in vivo. Whereas dipalmitoyl-phosphatidic acid is predominantly produced by PA treatment (53), a certain amount of arachidonic acid may be produced by repeated deacylation and reacylation at the *sn*-2 position and may contribute the phenotypes associated with FFA excess. However, a recent paper showed much weaker activation of stress molecules such as JNK by a variety of unsaturated FFAs, including arachidonic acid, compared with saturated FFAs (54), consistent with our results suggesting that saturated FFAs exert much stronger cytotoxicity compared with unsaturated FFAs.

Intracellular events associated with LPC-induced apoptosis are not clearly defined. Recent papers reported that GPCRs mediate various actions of LPC (33, 34), but it remains controversial whether GPCRs are LPC receptors or mediate LPC actions indirectly. The inhibition of PA- or LPC-induced Chang cell apoptosis by PTX or a dominant-negative $G\alpha_i$ mutant (18) suggests that certain GPCR/$G\alpha_i$ is involved in apoptosis by endogenous or exogenous LPC (55). The effect of a dominant-negative $G\alpha_i$ mutant observed in this study is not mediated by lysophosphatidic acid (LPA), which could be produced from LPC by autotaxin (56), because Chang cell death by PA or LPC was not inhibited by Ki16425, an LPA_1/LPA_3 receptor antagonist (56), and LPA up to 50 μM did not induce Chang cell death (M. S. Han et al., unpublished data). Furthermore, LPA is a well-known survival or growth factor and has been shown to protect cells from apoptosis (57).

Because GPCRs recognize extracellular ligands, LPC might be released to the extracellular space and bind to GPCRs (58). Instead, LPC might enter the receptor binding site in a lateral manner between transmembrane regions of the receptor without leaving the membrane (59), which is more consistent with the absence of the increase of LPC content in the culture supernatant after PA treatment. However, it is not proven whether such a model proposed for LPA is valid for LPC binding to its receptors. Downstream of receptor binding, we observed decreased cardiolipin content after PA treatment, consistent with a previous report (53). The PA-induced decrease in cardiolipin content could be attributable to the inhibition of CDP-DAG synthase, the rate-limiting step in cardiolipin biosynthesis, by LPC, as suggested previously (60). Although a different mechanism, such as poor substrate availability of dipalmitoyl-phosphatidic acid for CDP-DAG synthase, has been proposed (53), the inhibition of lipoapoptosis and the reversal of the decrease in cardiolipin content by PLA_2 inhibitors downstream of phosphatidic acid support a role for LPC rather than dipalmitoyl-phosphatidic acid upstream of PLA_2. The loss of cardiolipin, a mitochondria-specific phospholipid that maintains mitochondrial membrane stability by binding to cytochrome *c* (61), is probably responsible for cytochrome *c* translocation, the loss of mitochondrial potential, and cell death after PA treatment. Besides receptor binding, LPC might directly induce mitochondrial events by recruiting Bid, a well-known initiator of apoptosis, to the mitochondrial membrane (35). JNK activation by saturated FFAs may also contribute to the cytochrome *c* release and lipoapoptosis in hepatocytes, whereas the contribution of JNK activation in the lipoapoptosis of Chang cells does not appear to be dominant. Although we focused on the mitochondrial events associated with LPC accumulation in the course of hepatocyte death by PA, previous papers showed the involvement of other organelles, such as endoplasmic reticulum and lysosome, in the lipoapoptosis of hepatocytes (5–8). Further work will be required to address the potential relationship between the $iPLA_2$/LPC pathway and endoplasmic reticulum stress or lysosomal permeabilization (7, 8, 24).

The inability of OA to induce lipoapoptosis is consistent with JNK activation by saturated FFAs but not by unsaturated fatty acids (54). The increased TG content by OA but not by PA and the further increase by combined OA/PA treatment suggest that an increased channeling of PA into TG plays a protective role against PA-induced lipoapoptosis. Although channeling into TG protects against lipotoxicity, excessive TG may impose deleterious effects on cellular function, such as impaired insulin production in pancreatic β-cells. An increased TG content in the liver leads to steatosis, which is one of the two main features of NAFLD. The preferential increase of TG content by unsaturated fatty acids might be attributable to the increased stability of lipid droplets containing a higher percentage of unsaturated acyl chains (37).

The death of hepatocytes constitutes another main feature of NAFLD, leading to inflammation, fibrosis, and ultimately cirrhosis (NASH). Cells may enter the steatosis track if the DAG→TG pathway prevails or the death track if the DAG→PC→LPC pathway predominates, which might depend on the amount and types of available FFAs or the "second hit," such as inflammatory cytokines (62, 63), that may determine the conversion of steatosis to hepatitis (Fig. 8). Consistent with our in vitro models, we observed increased LPC content in patients with NAFLD depending on the severity of the disease, yet we cannot completely eliminate the possibility that the difference in the methods of tissue sampling between NAFLD tissue and control tissue might have affected the results. The development of hepatitis and increased liver enzymes after LPC administration also provides another line of in vivo evidence supporting the role of LPC in liver injury.